

The original 1990
hardcover edition

Privman

FINITE SIZE SCALING AND NUMERICAL
SIMULATION OF STATISTICAL SYSTEMS

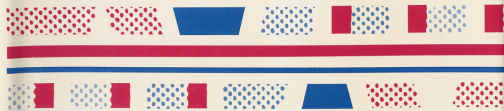
ISBN 981-02-0108-7



Finite Size Scaling and Numerical Simulation of Statistical Systems

Editor

V Privman



World Scientific

ISBN
981-02-0108-7

Softcover edition
(reprinted 1998)

Privman

Finite Size Scaling and
Numerical Simulation of Statistical Systems

ISBN 981-02-3796-0 (pbk)



http://www.worldscientific.com/



Finite Size Scaling and Numerical Simulation of Statistical Systems

Editor

V Privman



World Scientific

ISBN
981-02-3796-0

I. FINITE-SIZE SCALING THEORY

Vladimir Privman

TABLE of CONTENTS

1. Introduction	4
1.1. Opening remarks	4
1.2. Outline of the review	5
1.3. Basic scaling postulate	6
2. Finite-size scaling at critical points	11
2.1. Scaling ansatz for $d < 4$	11
2.2. RG and corrections to scaling	13
2.3. Finite-size scaling in the limit $\alpha \rightarrow 0$	15
2.4. Selection of metric factors	18
2.5. Nonperiodic boundary conditions	19
2.6. Surface and corner free energies	24
2.7. Finite-size properties of $d > 4$ systems	28
2.8. Other research topics	31
2.8.1. Microcanonical and fixed- M ensembles	31
2.8.2. Anisotropic models	32
2.8.3. Dynamics	32
2.8.4. Random systems	32

(continued)

"Finite-Size Scaling Theory," by V. Privman, Pages 1-98, Chapter I in
 "Finite Size Scaling and Numerical Simulation of Statistical Systems,"
 edited by V. Privman (World Scientific, Singapore, 1990)

3. Critical-point scaling: survey of results	33
3.1. Definitions and notation	33
3.1.1. Thermodynamic quantities	33
3.1.2. Binder's cumulant ratio	34
3.1.3. Types of surfaces (boundary conditions)	35
3.2. Results for cumulant and other ratios	36
3.2.1. Binder's cumulant ratio at T_c	36
3.2.2. Cumulant scaling asymptotics	38
3.2.3. High-order free energy derivative ratios at T_c	40
3.3. Free energy and correlation length scaling	41
3.3.1. Spherical model results	41
3.3.2. ϵ-expansion results	42
3.3.3. Numerical estimates of 3d amplitudes	43
3.3.4. Conformal invariance in 2d	44
3.3.5. Correlation lengths for $L \times \infty$ strips	44
3.3.6. Second-moment correlation length amplitudes in 2d	45
3.3.7. Tests of free energy scaling in 2d	46
3.3.8. Free energy amplitudes for systems with corners	47
4. Size effects on interfacial properties	48
4.1. Interfacial free energy near criticality	48
4.1.1. Periodic interfaces	48
4.1.2. Exact and numerical results for periodic interfaces	50
4.1.3. Pinned interfaces	51
4.1.4. Exact 2d Ising results for pinned interfaces	54
4.2. Interfacial free energy below criticality	54
4.3. Other research topics	56
4.3.1. Size effects on wetting	56
4.3.2. Fluctuating interfaces in cylindrical and slab geometries	57
4.3.3. Step free energy near roughening temperature	59

(continued)

5. First-order transitions	60
5.1. Opening remarks	60
5.2. Hypercubic Ising models at the phase boundary	60
5.3. Cubic n-vector models in the giant-spin approximation	62
5.3.1. Néel's mean-field theory of superparamagnetism	62
5.3.2. Giant-spin concept and discontinuity fixed point scaling	64
5.3.3. Upper critical dimension for first-order transitions	65
5.4. Crossover to cylindrical geometry: Ising case	66
5.4.1. Longitudinal correlation length	66
5.4.2. Calculation of the scaling functions	68
5.4.3. Cylindrical limit scaling	70
5.4.4. Size dependence of ξ_{\parallel} and RG scaling	71
5.4.5. Exact and numerical tests of scaling for Ising cylinders and cubes	73
5.5. Spin-wave effects for $n = 2, 3, \dots, \infty$	74
5.5.1. Cylinder-limit scaling	74
5.5.2. Spin waves in cubic geometries	76
5.5.3. Spherical model results	79
5.5.4. Quantum models	80
5.6. Nonsymmetric $n = 1$ transitions	80
5.6.1. General formulation	80
5.6.2. Two-phase coexistence	81
5.6.3. Probability distribution for the order parameter	83
5.6.4. Exact and transfer matrix results	85
5.7. Miscellaneous topics	85
5.7.1. Matching of scaling forms	85
5.7.2. Extension to nonperiodic boundary conditions	87
5.7.3. Loci of partition function zeros	87
6. Conclusion	88
Acknowledgements	88
References	88

FINITE-SIZE SCALING THEORY

Vladimir Privman

Department of Physics, Clarkson University
Potsdam, New York 13676, USA

1. INTRODUCTION

1.1. Opening Remarks

In this chapter we review the finite-size scaling theory of continuous phase transitions (critical points), as well as certain results on finite-size effects at first-order transitions, and also for systems with fluctuating interfaces. Studies of finite-size effects are important in interpreting experimental data and numerical results of Monte Carlo (MC) and transfer matrix calculations, and in connection with other theoretical developments, notably, conformal invariance and surface critical phenomena.

Our exposition will be biased towards numerical data analyses where a prototype finite-size system is d -dimensional hypercubic, L^d , or nearly hypercubic-shaped, or cylindrical, $L^{d-1} \times \infty$, (for transfer matrix studies). Much of our discussion will refer to the theoretically most studied case of *periodic boundary conditions* which are a

natural choice in many MC and transfer matrix applications. Results for other boundary conditions will be described, when available. While most of the considerations will be quite general, we will use the nomenclature of the ferromagnetic n -vector models on regular d -dimensional lattices. Note that transfer matrix calculations are usually performed in $d = 2$. Only recently, some $d = 3$ studies have been reported. On the other hand, MC calculations can be carried out in dimensionalities as high as $d = 5$ or 6.

1.2. *Outline of the Review*

As previously mentioned, this chapter is devoted to scaling theories of finite-size effects. Other chapters of this book cover calculational methods, *e.g.*, the Renormalization Group (RG) approach, and numerical applications.

Since the introduction of the finite-size scaling ideas by Fisher and co-workers in early seventies, several comprehensive expository and review articles have appeared covering both the original scaling ideas and later advancements, see, *e.g.*, [1-7]. Some of the important contributions have been reprinted in [8]. In the following subsection of the introduction (Sect. 1.3) a simple finite-size scaling ansatz [1] will be explained.

The modern form of the critical-point finite-size scaling [9], reviewed in Sect. 2, incorporates *hyperscaling* ideas and leads to the identification of universal finite-size critical-point amplitudes. Universal amplitudes and, more generally, universal quantities derivable from finite-size scaling functions have been estimated by numerical

MC, exact $2d$ conformal invariance, and numerical transfer matrix calculations. These studies are selectively surveyed in Sect. 3: a more comprehensive review can be found, *e.g.*, in [10].

Sections 4 and 5 are devoted, respectively, to interfacial finite-size properties, and to first-order transitions. Size effects on interfacial fluctuations (Sect. 4) both near T_c and below T_c , are quite diverse and have been studied relatively recently. Finite-size rounding of first-order transitions (Sect. 5) involves an interesting phenomenon of the emergence of characteristic finite-size length scales. Finally, brief summary remarks are given in Sect. 6.

1.3. Basic Scaling Postulate

Near the critical point at $t = 0$, $H = 0$, where

$$t \equiv (T - T_c) / T_c , \quad (1.1)$$

and H is the ordering field, various thermodynamic quantities diverge. The bulk ($L = \infty$) zero field critical behavior of, *e.g.*, the specific heat, $C(t, H; L)$, is given by

$$C_s(t, 0; \infty) \approx (A_{\pm}/\alpha)|t|^{-\alpha} , \quad (1.2)$$

where s denotes “singular part”, and the exponent α is included in the amplitudes for historical reasons. The standard scaling expression in nonzero field (see, *e.g.*, a review [11]) is

$$C_s(t, H; \infty) \approx |t|^{-\alpha} \mathcal{C}_{\pm} (H|t|^{-\Delta}), \quad (1.3)$$

where \mathcal{C}_{\pm} are certain scaling functions. As usual, in the above expressions the $+-$ refer to $t > 0$ and $t < 0$, respectively; the sign \approx indicates that corrections to scaling have been omitted. The exponents α and $\Delta = \beta + \gamma$ are universal, as is the ratio A_+/A_- . The full scaling functions \mathcal{C}_{\pm} can be made universal by introducing proper metric factors for t and H ; see Sect. 2.1-2.2 and further below.

For finite-size systems it has been recognized [1,12,13] that the system size L “scales” with the correlation length $\xi(t, H; \infty)$ of the bulk system. (Strictly speaking, this is only true in $d = 2, 3$, see Sect. 2.1.) Indeed, if $L \gg \xi(t, H; \infty)$, no significant finite-size effects should be observed. On the other hand, for $L \leq \xi(t, H; \infty)$, the system size will cut-off long-distance correlations so that an appreciable finite-size rounding of critical-point singularities is to be expected. Since the bulk correlation length scales similarly to (1.3),

$$\xi(t, H; \infty) \approx |t|^{-\nu} \Xi_{\pm} (H|t|^{-\Delta}), \quad (1.4)$$

the finite-size scaling combination is naturally $L/|t|^{-\nu}$. Thus one assumes

$$C_s(t, H; L) \approx |t|^{-\alpha} \tilde{\mathcal{C}}_{\pm} (H|t|^{-\Delta}; L|t|^{\nu}), \quad (1.5)$$

$$\xi(t, H; L) \approx |t|^{-\nu} \tilde{\Xi}_{\pm} (H|t|^{-\Delta}; L|t|^{\nu}), \quad (1.6)$$

with similar expressions for other quantities [1]. It is interesting to note that no new critical exponents were introduced in (1.5)-(1.6).

Relations (1.5)-(1.6) already yield many useful predictions, for example,

$$C_s(0, 0; L) \propto L^{\alpha/\nu} \quad \text{and} \quad \xi(0, 0; L) \propto L. \quad (1.7)$$

However, it turns out that additional rearrangement is quite useful. It involves four steps. Firstly, we use the so-called L -scaled instead of the t -scaled relations, *i.e.*, we redefine the scaling functions to have L enter in nonanalytic powers, while t and H enter linearly in combinations $tL^{1/\nu}$ and $HL^{\Delta/\nu}$. Secondly, we note that for a finite-size system there is actually no singularity at $t, H = 0$. Therefore, the scaling function will be smooth, analytic at the origin $tL^{1/\nu}, HL^{\Delta/\nu} = 0$. No distinct \pm functions are needed. The third step is to allow for nonuniversal metric factors for t and H , by using scaling combinations $a t L^{1/\nu}$ and $b H L^{\Delta/\nu}$. Then the scaling functions will be universal. It turns out that no metric factor is needed for L , see [9]. This issue will be further explored in Sect. 2.1-2.2. The final point is to use *free-energy density*, f , measured per $k_B T$, instead of the specific heat. Note that in terms of the singular parts, we have a simple relation

$$C_s = -k_B \frac{\partial^2 f_s}{\partial t^2} \quad . \quad (1.8)$$

Various thermodynamic quantities follow from the free energy by differentiation.

After carrying out all the above redefinitions, and making use of the hyperscaling relation

$$2 - \alpha = d\nu \quad (1.9)$$

in the free-energy expression, we end up with

$$f_s(t, H; L) \approx L^{-d} Y\left(atL^{1/\nu}, bHL^{\Delta/\nu}\right), \quad (1.10)$$

$$\xi(t, H; L) \approx LX\left(atL^{1/\nu}, bHL^{\Delta/\nu}\right), \quad (1.11)$$

where the scaling functions X and Y are universal [9]: see also Sect. 2.1.

We did not actually detail the transformation from (1.5)-(1.6) to (1.10)-(1.11). The reason is that it is much easier to proceed from (1.10)-(1.11) back to (1.5)-(1.6). Thus, for instance, for ξ we put

$$\tilde{\Xi}_{\pm}(z_1; z_2) = z_2 X\left(\pm az_2^{1/\nu}, bz_1 z_2^{\Delta/\nu}\right), \quad (1.12)$$

with a similar somewhat more complicated relation for \tilde{C}_{\pm} . Note that the precise choice of the metric factors $a > 0$ and $b > 0$ is not specified at this stage. They will be discussed in Sect. 2.4.

Relations (1.10)-(1.11) are convenient for deriving the behavior *at the critical point*. Thus, we have

$$f_s(0, 0; L) \approx Y(0, 0)L^{-d}, \quad (1.13)$$

$$\xi(0, 0; L) \approx X(0, 0)L, \quad (1.14)$$

involving two *universal amplitudes*, and also

$$C_s(0, 0; L) \approx -k_B a^2 \left[\frac{\partial^2 Y(\tau, \omega)}{\partial \tau^2} \right]_{\tau, \omega=0} L^{\alpha/\nu}, \quad (1.15)$$

etc.

The behavior in the bulk limit of $L \rightarrow \infty$ with $(t, H) \not\equiv (0, 0)$ is less apparent in (1.10)-(1.11). For example, for the free energy we obtain the bulk t -scaled scaling relation by requiring that

$$Y(\tau, \omega) \approx (\pm \tau)^{d\nu} Q_{\pm} (\omega (\pm \tau)^{-\Delta}), \quad \text{for } \tau \rightarrow \pm \infty, \quad (1.16)$$

where the functions Q_{\pm} are universal. This limiting behavior of Y implies

$$f_s(t, H; \infty) \approx a^{2-\alpha} |t|^{2-\alpha} Q_{\pm} (ba^{-\Delta} H |t|^{-\Delta}), \quad (1.17)$$

which is the usual bulk scaling law, with metric factors a and b making the scaling functions universal, and with $2 - \alpha = d\nu$ “built in”. Relation (1.3) is implicit in (1.17), via (1.8). The expression for C_{\pm} is, however, cumbersome and is not given here.

If the finite-size system is sufficiently high-dimensional to have its own critical point, as happens, *e.g.*, for $L \times \infty^2$ Ising “slabs” in 3d, then this will be manifested by a singularity of $Y(\tau, \omega)$ and $X(\tau, \omega)$

at $\tau = \tau_0 \neq 0$, $\omega = 0$, see [1-2] for further discussion and references. For L^d and $L^{d-1} \times \infty$ systems one can define an *apparent shifted critical point*, *e.g.*, by a location of the specific heat maximum. Thus, we solve for τ_0 in

$$\left[\frac{\partial^3 Y(\tau, \omega)}{\partial \tau^3} \right]_{\tau=\tau_0, \omega=0} = 0. \quad (1.18)$$

The value τ_0 is universal. The apparent critical temperature shift is then given by

$$t_0 = a^{-1} \tau_0 L^{-1/\nu}. \quad (1.19)$$

2. FINITE-SIZE SCALING AT CRITICAL POINTS

2.1. Scaling Ansatz for $d < 4$

In this subsection we consider systems below the upper critical dimension d_c [11], where $d_c = 4$ for n -vector models. We also assume no logarithmic singularities, that is, we assume $\alpha \neq 0, -1, -2, \dots$. For systems with *periodic boundary conditions* it has been established by heuristic scaling [9,14-15], as well as by explicit RG calculations [5,16-18], that the system size L enters with no corresponding metric factor, *i.e.*, as a macroscopic length scale leading naturally to relations (1.10)-(1.11). Thus the metric factors a and b contain all the nonuniversal system-dependent aspects of the leading critical behavior. More generally, the boundary conditions and system

shape are also “macroscopic” geometric features in the sense that the scaling functions Y and X depend on the geometry.

For the free energy it is important to also consider the nonsingular “background” which can be chosen to have no field dependence,

$$f(t, H; L) = f_s(t, H; L) + f_{ns}(t; L). \quad (2.1)$$

Recent studies [5,9,14-18] indicate that for periodic boundary conditions one can assume $f_{ns}(t; L) = f_{ns}(t; \infty)$. For other boundary conditions, the background may lead to new interesting finite-size features (see below).

As already noted in deriving (1.17) from (1.10), the hyperscaling relation (1.9) is implicit in (1.10). In fact, relations (1.10)-(1.11) are rather strong forms of the scaling-with-hyperscaling postulate incorporating various properties which are known to hold for $d < 4$ within the RG formalism: they include the equality of critical exponents for $t < 0$ and $t > 0$; the use of the same metric factors for f_s and ξ ; hyperscaling exponent relations; and the so-called two-scale-factor universality or hyperuniversality relations among critical point amplitudes [10]. The last property is of particular interest and warrants further discussion.

Consider the zero-field relation (1.17),

$$f_s(t, 0; \infty) \approx a^{d\nu} q_{\pm} |t|^{2-\alpha}, \quad (2.2)$$

where $q_{\pm} = Q_{\pm}(0)$ are universal. By considering the equivalent of (1.16) for the correlation length scaling function, we can also derive

the relation

$$\xi(t, 0; \infty) \approx a^{-\nu} k_{\pm} |t|^{-\nu}, \quad (2.3)$$

where k_{\pm} are universal. We thus find that for small t , the $t > 0$ and $t < 0$ combinations

$$f_s(t \rightarrow 0^{\pm}, 0; \infty) \xi^d(t \rightarrow 0^{\pm}, 0; \infty) = q_{\pm} k_{\pm}^d \quad (2.4)$$

have universal constant limiting values. This is just the standard statement of hyperscaling [19-20] based on the hypothesis that for strongly fluctuating (non-mean-field) critical behavior there is a single divergent “macroscopic” length scale, ξ . The singular free energy in volume ξ^d is then a universal multiple of $k_B T_c$. The finite-size equivalent of this hypothesis [9] are relations (1.13)-(1.14), and more generally, the observation that the ratio of the “macroscopic” lengths L and ξ entails no new “microscopic” metric factor.

2.2. RG and Corrections to Scaling

The RG interpretation of the L -scaled relations (1.10)-(1.11) is particularly transparent. Indeed, the exponents of L in the scaling combinations, are just the *relevant* eigenexponents

$$\lambda_t = \frac{1}{\nu} > 0 \quad \text{and} \quad \lambda_H = \frac{\Delta}{\nu} > 0, \quad (2.5)$$

corresponding to the scaling fields [21] of the RG transformation,

$$g_t = al^{\lambda_t} t + o(t, H), \quad (2.6)$$

$$g_H = bl^{\lambda_H} H + o(t, H). \quad (2.7)$$

We introduced an arbitrary *fixed* (system independent) microscopic length scale l to have L enter in a dimensionless ratio when (1.10)-(1.11) are rewritten in terms of g_t and g_H ,

$$f_s(t, H; L) \approx L^{-d} Y [g_t(L/l)^{\lambda_t}, g_H(L/l)^{\lambda_H}], \quad (2.8)$$

$$\xi(t, H; L) \approx LX [g_t(L/l)^{\lambda_t}, g_H(L/l)^{\lambda_H}]. \quad (2.9)$$

Note that we did not care to define H in dimensionless units. One can always chose b to have g_H dimensionless.

The RG relations (2.8)-(2.9) are actually more basic than the phenomenological scaling forms (1.10)-(1.11), and they can be extended to include arguments for additional relevant ($\lambda > 0$) scaling fields in the cases of *multicritical phenomena*, or associated with *surface couplings*.

Corrections to scaling result from the nonlinearity of the scaling fields $g(t, H)$ [*i.e.*, the $o(t, H)$ corrections in (2.6)-(2.7)], as well as from including additional arguments in (2.8)-(2.9) for the *irrelevant* ($\lambda < 0$) scaling fields. For finite-size systems only the leading irrelevant-variable correction to scaling contribution has been considered in detail in the literature and estimated numerically [22]. Let

θ denote the leading bulk correction to scaling exponent associated with the irrelevant RG field $g_u(t, H)$, taking the finite value uL^{λ_u} at $t = 0, H = 0$, with eigenexponent

$$\lambda_u = -\frac{\theta}{\nu} < 0. \quad (2.10)$$

Then the scaling relation (1.11) for ξ for instance, is replaced by

$$\xi \approx L\bar{X}\left(atL^{1/\nu}, bHL^{\Delta/\nu}; uL^{-\theta/\nu}\right), \quad (2.11)$$

which in turn can be expanded in the third argument to isolate the leading correction to scaling contribution due to the irrelevant variable g_u ,

$$\xi \approx LX\left(atL^{1/\nu}, bHL^{\Delta/\nu}\right) + uL^{1-\frac{\theta}{\nu}}X_u\left(atL^{1/\nu}, bHL^{\Delta/\nu}\right). \quad (2.12)$$

The scaling functions \bar{X} and X_u are universal. However, the correction term has the “front” nonuniversal coefficient u . A similar construction is possible for the free energy. For a systematic study of the bulk “nonlinear” and “irrelevant” corrections to scaling, and their interplay, consult [10,23].

2.3. Finite-Size Scaling in the Limit $\alpha \rightarrow 0$

Consider first the bulk zero-field critical-point free energy,

$$f_s(t; L = \infty) \approx F_{\pm}|t|^{2-\alpha}, \quad (2.13)$$

where we omitted the H -dependence ($H = 0$) for simplicity. We have

$$F_{\pm} = a^{2-\alpha} q_{\pm}, \quad (2.14)$$

see (2.2). Also, we expand $f_{ns}(t; \infty)$ about $t = 0$,

$$f_{ns}(t; \infty) = F_0 + F_1 t + F_2 t^2 + o(t^2). \quad (2.15)$$

As $\alpha \rightarrow 0$, poles develop in F_{\pm} and F_2 , yielding a logarithmic specific heat singularity: see, *e.g.*, [24] where similar effects for $\alpha \rightarrow -1, -2, -3, \dots$, are also described. Thus, we have

$$q_{\pm} = -\frac{q_0}{\alpha} + \bar{q}_{\pm} + O(\alpha), \quad (2.16)$$

with universal $q_0 > 0$ and \bar{q}_{\pm} . Also, we have

$$F_2 = a^{2-\alpha} \frac{q_0}{\alpha} + \bar{F}_2 + O(\alpha), \quad (2.17)$$

so that the terms in α^{-1} cancel out. Collecting terms and assuming that F_0 and F_1 remain finite as $\alpha \rightarrow 0$, we get the leading terms in the free energy in the form

$$f(t; \infty) \approx F_0 + F_1 t + [\bar{F}_2 + a^2 \bar{q}_{\pm}] t^2 + a^2 q_0 t^2 \ln |t|. \quad (2.18)$$

Thus, the leading singular behavior of the free energy consists of the $t^2 \ln |t|$ and discontinuous t^2 contributions.

Extension of the above mechanism to finite-size systems with *periodic boundary conditions* (and $H = 0$) was proposed in [25]. Since the nonsingular background (2.15), with (2.17), remains the same for $L < \infty$, the α^{-1} divergence in (2.17) must be compensated for by a contribution from the scaling part,

$$f_s \approx L^{-d} Y(atL^{1/\nu}, 0). \quad (2.19)$$

As $\alpha \rightarrow 0$, we have

$$Y(\tau, 0) = -\frac{q_0}{\alpha} |\tau|^{2-\alpha} + \bar{W}_\pm(\tau) + O(\alpha), \quad (2.20)$$

which, after some algebra, yields the $\alpha = 0$ result

$$f(t; L) \approx f(t; \infty) + L^{-d} \bar{W}_\pm(atL^{d/2}), \quad (2.21)$$

where $f(t; \infty)$ is given by (2.18), and we used (1.9) with $\alpha = 0$. Because the leading term in (2.20) is nonanalytic in τ , however, we have to use separate scaling functions \bar{W}_\pm for $\tau > 0$ and $\tau < 0$.

According to [25], a smooth finite-size scaling function can be defined at the expense of separating out logarithmic size dependence as follows,

$$f(t; L) \approx F_0 + F_1 t + \left[-a^2 q_0 \ln(aL^{d/2}) + \bar{F}_2 \right] t^2 + L^{-d} W(atL^{d/2}). \quad (2.22)$$

The connection is given by

$$\bar{W}_\pm(\tau) = W(\tau) - \bar{q}_\pm \tau^2 - q_0 \tau^2 \ln(\pm\tau). \quad (2.23)$$

2.4. Selection of Metric Factors

In this subsection we again consider zero-field critical behavior and discuss in detail the procedure for fixing the metric factor a entering various scaling relations introduced above. The discussion can in principle be extended to any other *relevant* scaling variable, *e.g.*, H , and the appropriate metric factor relating it to the RG scaling field [see (2.6)-(2.7)].

Consideration of relations (2.13)-(2.14), (2.19), as well as the $\alpha \simeq 0$ relations (2.17)-(2.18), indicates that $a^{2-\alpha}$ measures an overall nonuniversal free-energy scale or “strength” of, *e.g.*, the bulk $|t|^{2-\alpha}$ singularity, while all other parameters, including the bulk exponent α and amplitude ratio F_+/F_- , are universal and depend only on the universality class. Finite-size universal quantities, like $Y(\tau, 0)$, depend also on geometry (shape, and boundary conditions). The selection of a is actually quite arbitrary. It is convenient to define it in terms of the bulk parameters F_\pm and α in order to have no geometry dependence. A particular choice of a implies certain restrictions on the universal scaling-function-related quantities which can be imposed without violating any of the general universality properties discussed in the preceding subsections. For example, if we take $a^{2-\alpha} = |F_+|$, then $q_+ = \text{sign}(F_+)$. We could also take $a^{2-\alpha} = |F_-|$, implying $q_- = \text{sign}(F_-)$, or a symmetric choice $a^{2-\alpha} = |F_+ + F_-|$, implying $q_+ + q_- = \text{sign}(F_+ + F_-)$, *etc.*

However, in some models $F_+ = 0$ while $F_- \neq 0$, or vice-versa. Similarly, F_\pm diverge as $\alpha \rightarrow 0$. In fact, all three definitions mentioned in the preceding paragraph are inappropriate in certain cases. The guidance for a proper definition of a symmetric free-energy scale comes from a rather unexpected source: study of the complex- t plane zeros of the partition function,

$$Z(t, H = 0; L) = e^{-V f(t, 0; L)}, \quad (2.24)$$

and the connection between the location of these zeros and the finite-size scaling relation (2.19). The following “natural” definition,

$$a = [F_+^2 + F_-^2 - 2F_+F_- \cos(\pi\alpha)]^{\frac{1}{2(2-\alpha)}}, \quad (2.25)$$

emerges in these studies [26] which are rather complicated and are not reviewed here. When a is defined by (2.25), it can be shown that it remains finite (nondivergent and nonzero) in all the “pathological” cases like $\alpha \rightarrow 0$, etc. Note that (2.25) implies the following relation among the universal scaling function coefficients,

$$q_+^2 + q_-^2 - 2q_+q_- \cos(\pi\alpha) = 1. \quad (2.26)$$

2.5. Nonperiodic Boundary Conditions

In this subsection we consider systems with *free boundary conditions* and review recent finite-size scaling results [27-29]. Extensions to other boundary conditions (e.g., fixed, etc.) are quite straight-

forward. For simplicity, we put $H = 0$ in this subsection, and we restrict our discussion to the case of flat surfaces. With these restrictions, one can fully illustrate the new finite-size effects involved. Thus, we consider systems with flat surfaces, straight edges, and corners, in $3d$, and straight-edge polygons in $2d$. Extension to curved boundaries is also possible [27-28].

Consider first finite-size behavior away from T_c when the bulk correlation length,

$$\xi^{(b)} \equiv \xi(t; L = \infty), \quad (2.27)$$

is small compared to a characteristic system size L . For systems with no soft modes (spin waves), which we assume here for simplicity, it has been well established [1-2] that the free energy (and other thermodynamic quantities) can be expanded as

$$\begin{aligned} f(t; L) - f^{(b)}(t) &= \frac{1}{L} f^{(s)}(t) + \frac{1}{L^2} f^{(e)}(t) + \frac{1}{L^3} f^{(c)}(t) \\ &\quad + O\left(e^{-L/\xi^{(b)}}\right), \quad (d = 3), \end{aligned} \quad (2.28)$$

$$f(t; L) - f^{(b)}(t) = \frac{1}{L} f^{(s)}(t) + \frac{1}{L^2} f^{(c)}(t) + O\left(e^{-L/\xi^{(b)}}\right), \quad (d = 2), \quad (2.29)$$

where

$$f^{(b)} \equiv f(t; \infty) \quad (2.30)$$

is the bulk free energy. The contributions proportional to $f^{(s)}$, $f^{(e)}$ and $f^{(c)}$ are attributed to surfaces, edges (in 3d) and corners.

The bulk free energy $f^{(b)}(t)$ is the same for all boundary conditions. For each type of surface, one can define the surface free energy density, $f^{(\text{surface})}$, (measured per $k_B T$ and per unit surface area). Similarly, one can define the edge free energy for each type of edge, $f^{(\text{edge})}$, specified by the opening angle and types of adjacent surfaces (and measured per $k_B T$ and per unit length). Finally, for each corner, one can specify the corner free energy, $f^{(\text{corner})}$, depending on the corner type (number of edges, opening angles, types of surfaces, and measured per $k_B T$). Unlike $f^{(s)}$, $f^{(e)}$, $f^{(c)}$, the quantities $f^{(\text{surface})}$, $f^{(\text{edge})}$, $f^{(\text{corner})}$ depend only on the *local* geometry. These free energies are related up to sample shape dependent proportionality factors. For 3d slabs, $L \times \infty^2$, with free boundary conditions, we have $f^{(s)} = 2f^{(\text{surface})}$ with $f^{(e)} = 0$, $f^{(c)} = 0$. Similar relations apply for 2d strips. For 3d cylinders with a square cross-section, $L^2 \times \infty$, we have $f^{(s)} = 4f^{(\text{surface})}$, $f^{(e)} = 4f^{(\text{edge})}$, $f^{(c)} = 0$. For 3d cubes, L^3 , we have $f^{(s)} = 6f^{(\text{surface})}$, $f^{(e)} = 12f^{(\text{edge})}$, $f^{(c)} = 8f^{(\text{corner})}$, while for 2d squares, L^2 , we have $f^{(s)} = 4f^{(\text{surface})}$, $f^{(c)} = 4f^{(\text{corner})}$, etc. We will return to some of these relations in the next subsection.

Concerning the behavior near T_c , there is accumulating numerical and analytical evidence, reviewed in part in Sect. 3, that the *nonsingular part* $f_{ns}(t; L)$ has an expansion similar to (2.28)-(2.29). For example, in 2d,

$$f_{ns}(t; L) = f_{ns}^{(b)}(t) + \frac{1}{L} f_{ns}^{(s)}(t) + \frac{1}{L^2} f_{ns}^{(c)}(t) + o(L^{-2}). \quad (2.31)$$

For the leading scaling of the *singular part* of the free energy in general $d < 4$, let us tentatively accept the form (2.19), although later we will find that modifications are necessary in some instances. The $o(L^{-2})$ corrections in (2.31) and similar terms, $o(L^{-3})$, in $3d$, are expected to be $\sim L^{-(d+1)}$, etc., ($d = 2, 3$). However, the leading “geometry-associated” terms in the expansion of $f_{ns}(t; L)$ closely parallel the series (2.28)-(2.29). For example, for slabs or strips, as mentioned above, we anticipate that the edge and corner terms are not present, *i.e.*, only $f_{ns}^{(s)}$ is nonzero. To the extent that they are available, the field-theoretical ϵ -expansion results for nonperiodic finite-size systems [30-32] substantiate this phenomenological expectation which we already encountered in its simplest form when assuming $f_{ns}(t; L) \cong f_{ns}(t; \infty)$ for periodic boundary conditions. Presently, the field-theoretical studies are, however, limited due partly to difficulties in treating nonuniform order parameter profiles below T_c .

For systems with corners, the expansions of the form (2.31) have all the “geometry” terms present, which are proportional to inverse *integral* powers of $1/L$. On the other hand, the scaling term (2.19) is proportional to $1/L^d$ with, generally, varying d . When d passes through integer values 2 or 3, we anticipate “resonant” divergences in Y and $f_{ns}^{(c)}$ yielding logarithmic terms [27], reminiscent of the mechanism of logarithmic specific heat as $\alpha \rightarrow 0$ (Sect. 2.3). Thus, in the limit $d \rightarrow D = 2$ or 3, we take

$$Y(\tau, \omega) = \frac{y}{D-d} + \tilde{Y}(\tau, \omega) + O(d-D),$$

$$f_{ns}^{(c)}(t) = \frac{yl^{D-d}}{d-D} + \tilde{f}_{ns}^{(c)}(t) + O(d-D), \quad (2.32)$$

where for completeness we restored the magnetic-field dependence (second argument, ω , in Y). As before, l is a microscopic length which can be completely arbitrary here. (In Sect. 2.52 we required l to be system-independent. Here one can take, *e.g.*, $l = a^{-\nu}$.) After some algebra, one gets

$$\begin{aligned} f(t, H; L) \approx & L^{-3} \tilde{Y}\left(atL^{1/\nu}, bHL^{\Delta/\nu}\right) + yL^{-3} \ln(L/l) \\ & + f_{ns}^{(b)}(t) + \frac{1}{L} f_{ns}^{(s)}(t) + \frac{1}{L^2} f_{ns}^{(e)}(t) + \frac{1}{L^3} \tilde{f}_{ns}^{(c)}(t), \quad (d=3), \end{aligned} \quad (2.33)$$

$$\begin{aligned} f(t, H; L) \approx & L^{-2} \tilde{Y}\left(atL^{1/\nu}, bHL^{\Delta/\nu}\right) + yL^{-2} \ln(L/l) \\ & + f_{ns}^{(b)}(t) + \frac{1}{L} f_{ns}^{(s)}(t) + \frac{1}{L^2} f_{ns}^{(c)}(t), \quad (d=2), \end{aligned} \quad (2.34)$$

where both the scaling function $\tilde{Y}(\tau, \omega)$ and the coefficient y are universal. Both depend on the universality class, *i.e.*, dimensionality, symmetry, *etc.*, but also, as is usual for finite-size systems, on the precise geometry and boundary conditions.

Thus far the scaling predictions (2.33)-(2.34) have been tested [28-29] only at T_c , as reviewed in Sect. 3.3.8 below. The universal and nonuniversal contributions L^{-D} cannot be separated at T_c , but one can study the $yL^{-D} \ln L$ term.

In fact, relations (2.33)-(2.34) apply generally to systems with curved boundaries [27-28] or in curved-space geometries. The amplitude y is then a global property [28]. However, if the only source of the $yL^{-D} \ln L$ contribution are *corners*, with otherwise flat geometry and boundaries, then one can attribute $y^{(\text{corner})}$ to each corner [28] (see also Sect. 3), so that

$$y = \sum_{\text{corners}} y^{(\text{corner})}. \quad (2.35)$$

Universal terms proportional to $L^{-d} \ln L$ also arise in Gaussian models [28] which were investigated only for integer d (see Sect. 4.2). However, the mechanism of their emergence described above is not applicable in this case, in the least because the finite-size scaling form (1.10) does not apply.

2.6. Surface and Corner Free Energies

Consider again systems with nonperiodic boundary conditions, flat surfaces, and $H = 0$, so that relations (2.28)-(2.29) apply away from T_c , *i.e.*, when $L \rightarrow \infty$ for fixed $t \neq 0$. These expansions define the functions $f^{(s)}$, $f^{(e)}$, $f^{(c)}$, which in turn are related to $f^{(\text{surface})}$, $f^{(\text{edge})}$, $f^{(\text{corner})}$, with geometry-dependent rules relating the two sets, as explained in Sect. 2.5. After taking the $L \rightarrow \infty$ limit for fixed $t \neq 0$, one can still consider the critical-point behavior of all the above free energies as $|t| \rightarrow 0$. For brevity we take $t \rightarrow 0^+$ here.

Singular contributions to the free energies can also be evaluated by considering the asymptotic form of the scaling function $\tilde{Y}(\tau, 0)$

in (2.33)-(2.34) for large positive τ , *i.e.*, in the regime $L >> (at)^{-\nu}$, or equivalently, $L >> \xi^{(b)}$. A standard argument [27] suggests

$$\tilde{Y}(\tau, 0) \approx y_3 \tau^{3\nu} + y_2 \tau^{2\nu} + y_1 \tau^\nu - \nu y \ln \tau + y_0 + \dots, \quad (3d),$$

$$\tilde{Y}(\tau, 0) \approx y_2 \tau^{2\nu} + y_1 \tau^\nu - \nu y \ln \tau + y_0 + \dots, \quad (2d),$$

where the coefficients are universal and geometry dependent, except for $y_d \equiv q_+$. One thus obtains the standard results [1] [see also (2.2)]

$$f_s^{(b)}(t) \approx q_+ (at)^{d\nu} \quad \text{and} \quad f_s^{(s)}(t) \approx y_{d-1} (at)^{(d-1)\nu}, \quad (2.38)$$

as well as less familiar relations [27]

$$f_s^{(e)}(t) \approx y_1 (at)^\nu \quad \text{in} \quad 3d, \quad (2.39)$$

$$f_s^{(c)}(t) \approx -\nu y \ln |t|, \quad d = 2 \text{ or } 3, \quad (2.40)$$

where for completeness we also included the appropriate $t < 0$ expression in the leading order “corner” result (2.40).

Consideration of the connection between the set of coefficients $f^{(s)}$, $f^{(e)}$, $f^{(c)}$, and the surface, edge, corner free energies further leads to the conclusions that as $t \rightarrow 0^\pm$,

$$f_s^{(\text{surface})} \approx q_{\pm}^{(\text{surface})} |at|^{(d-1)\nu}, \quad (d = 2, 3), \quad (2.41)$$

$$f_s^{(\text{edge})} \approx q_{\pm}^{(\text{edge})} |at|^{(d-2)\nu}, \quad (d = 3), \quad (2.42)$$

$$f_s^{(\text{corner})} \approx -\nu y^{(\text{corner})} \ln |t|, \quad (d = 2, 3), \quad (2.43)$$

where the universal coefficients $q_{\pm}^{(\text{surface})}$, $q_{\pm}^{(\text{edge})}$ and $y^{(\text{corner})}$ depend only “locally” on the type of the surface boundary conditions, edge and corner shape and angles, *etc.*, but they do not depend on the global geometry. Examination of the series (2.36)-(2.37) suggests that the corner free energy, for each corner, can be written as

$$f^{(\text{corner})}(t) \approx -\nu y^{(\text{corner})} \ln |t| + \phi_0 + q_{\pm}^{(\text{corner})}, \quad \text{for } t \rightarrow 0^{\pm}, \quad (2.44)$$

where the subleading constant terms are different for $t > 0$ and $t < 0$, with nonuniversal ϕ_0 , but universal difference $q_+^{(\text{corner})} - q_-^{(\text{corner})}$. Relation (2.40) can be extended similarly because for a given flat-surface sample,

$$f^{(c)}(t) = \sum_{\text{corners}} f^{(\text{corner})}(t) \quad . \quad (2.45)$$

One can *define* [33] surface, edge, corner free energies by postulating that expansions (2.28)-(2.29) can be formally applied in the

critical region. Consider, for illustration [33], 3d boxes of size $L \times \bar{L}^2$, with periodic boundary conditions in the \bar{L} directions. In the direction of L we impose periodic (p) or free (f) boundary conditions. We then employ (2.28) to write

$$f(t; L) \simeq f^{(b)}(t), \quad (p), \quad (2.46)$$

$$f(t; L) \simeq f^{(b)}(t) + \frac{1}{L} f^{(s)}, \quad (f), \quad (2.47)$$

and we further employ the relation $f^{(s)} = 2f^{(\text{surface})}$, appropriate for the (f) geometry, to write

$$f(t; L) \simeq f^{(b)}(t) + \frac{2}{L} f^{(\text{surface})}, \quad (f). \quad (2.48)$$

Thus, we can define

$$f^{(\text{surface})}(t; L) \equiv \frac{L}{2} [f_{(f)}(t; L) - f_{(p)}(t; L)], \quad (2.49)$$

and use this definition even at T_c . The singular behavior of this quantity follows from those of $f_{(f)}$ and $f_{(p)}$,

$$f_s^{(\text{surface})}(t; L) \approx L^{-(d-1)} Y^{(\text{surface})} \left(atL^{1/\nu} \right), \quad (2.50)$$

where

$$2Y^{(\text{surface})}(\tau) \equiv [Y_{(f)}(\tau, 0) - Y_{(p)}(\tau, 0)]. \quad (2.51)$$

Note, however, that $f^{(\text{surface})}(t; L)$ thus defined [and similarly, for $f^{(\text{edge})}(t; L)$, etc.] will depend on the original reference geometries, except in the strict $L \rightarrow \infty$ limit (i.e., $|\tau| \gg 1$), when they reduce to $f^{(\text{surface})}(t)$, etc., considered before.

2.7. Finite-Size Properties of $d > 4$ Systems

For $d > 4$, finite-size scaling in its simple form described in Sect. 1.3 breaks down, as first noted in [14]. As with bulk critical behavior, the basic mechanism has been identified [4,34] as due to a dangerous irrelevant variable [35]. The RG scaling relations, compare (2.11) for ξ , apply:

$$f_s(t, H; L) \approx L^{-d} \bar{Y} \left(atL^2, bHL^{(d+2)/2}; uL^{4-d} \right), \quad (2.52)$$

$$\xi(t, H; L) \approx L \bar{X} \left(atL^2, bHL^{(d+2)/2}; uL^{4-d} \right), \quad (2.53)$$

where we used the RG eigenexponents

$$\lambda_t = 2, \quad \lambda_H = \frac{d+2}{2}, \quad \lambda_u = 4 - d, \quad (2.54)$$

at the Gaussian fixed point, and the irrelevant variable $u > 0$ is proportional to the coefficient of the fourth-order term in the Ginzburg-Landau Hamiltonian. However, the scaling functions $\bar{Y}(\tau, \omega; \rho)$ and $\bar{X}(\tau, \omega; \rho)$ are singular as $\rho \rightarrow 0$ and cannot be expanded in powers of ρ .

The most studied case is that of a nearly-hypercubic sample with periodic boundary conditions. Sum-rule [34] and heuristic [4] arguments, as well as constant order parameter mean-field [5,16] calculations, suggest that as $\rho \rightarrow 0$,

$$\bar{Y}(\tau, \omega; \rho) \approx \mathcal{P}\left(\tau\rho^{-\frac{1}{2}}, \omega\rho^{-\frac{1}{4}}\right). \quad (2.55)$$

Introducing nonuniversal constants

$$\bar{a} = au^{-\frac{1}{2}} \quad \text{and} \quad \bar{b} = bu^{-\frac{1}{4}}, \quad (2.56)$$

we then have

$$f_s(t, H; L) \approx L^{-d} \mathcal{P}\left(\bar{a}tL^{d/2}, \bar{b}HL^{3d/4}\right). \quad (2.57)$$

Thus, a universal two-variable scaling function suffices in this case (periodic cubes) and, in fact, \mathcal{P} can be obtained as a quadrature from the constant order parameter mean-field theory [5,16]. The correlation length scaling has been investigated in lesser detail [34]. Moment definitions of the correlation length [34] for finite samples, usually have a built in bound $\xi(t, H; L) \leq (\text{const } L)$, so that it is natural to conjecture that

$$\xi(t, H; L) \approx L\mathcal{R}\left(\bar{a}tL^{d/2}, \bar{b}HL^{3d/4}\right). \quad (2.58)$$

However, this conjecture has not been generally substantiated. In fact, the correlation length scaling is expected to be very sensitive to the precise definition of ξ .

For near-cubic systems with free boundary conditions, finite-size behavior of the free energy for $d > 4$ has been investigated within the mean-field type Gaussian approach [36]. While the general relation (2.52) seems to apply, one no longer has a simple pattern of a singular dependence on ρ , as in (2.55).

In the periodic cylinder geometry, $L^{d-1} \times \infty$, there are indications [4-5] that (2.55) is replaced by

$$\bar{Y}(\tau, \omega; \rho) \approx \rho^{1/3} \tilde{\mathcal{P}}\left(\tau \rho^{-2/3}, \omega \rho^{-1/2}\right), \quad (2.59)$$

$$\bar{X}(\tau, \omega; \rho) \approx \rho^{-1/3} \tilde{\mathcal{R}}\left(\tau \rho^{-2/3}, \omega \rho^{-1/2}\right), \quad (2.60)$$

where the correlation length is defined by the leading transfer matrix spectral gap. Among the various predictions that follow, we note that

$$\xi(0, 0; L) \approx u^{-1/3} \tilde{\mathcal{R}}(0, 0) L^{(d-1)/3}, \quad (2.61)$$

where $\tilde{\mathcal{R}}(0, 0)$ is universal, and $d > 4$. Additional results for $d > 4$ spherical models in various geometries will be mentioned in Sect. 3.

For $d = 4$, i.e., at the upper marginal dimensionality, one anticipates [5,14,16] logarithmic correction factors to the ordinary ($d < 4$) scaling laws. Explicit results are generally limited, and one has to evaluate finite-size quantities numerically [16].

2.8. *Other Research Topics*

In the preceding subsections, we described the theoretical foundations of the finite-size scaling description of static, isotropic critical behavior in prototype short-range n -vector models for $d < 4$, and we also outlined some results for $d > 4$. Here, for completeness, we list several other recently active research topics. We do not provide a detailed survey of these developments, but mostly list the relevant literature.

2.8.1. Microcanonical and Fixed- M Ensembles

Finite-size scaling in the *microcanonical* ensemble, where the system energy is the controlled variable, instead of the temperature, has been developed in [37], with an emphasis on applications in MC data analyses.

The magnetization density, $M(t, H; L)$, is obtained from the free energy via

$$M \equiv -k_B T \frac{\partial f}{\partial H}. \quad (2.62)$$

Study of finite-size effects in the fixed- M ensemble, *i.e.*, with system properties considered as functions of $(t, M; L)$, has been reported in [38-39]. Hyperuniversality of the scaling functions has been emphasized in [39].

2.8.2. Anisotropic Models

Finite-size behavior of anisotropic (directed) models has some interesting new aspects due to different correlation length divergence along different sample dimensions, and also due to the emergence, in some cases, of characteristic size-dependent length scales which diverge in the bulk limit even for $t \neq 0$. A comprehensive summary of various results and concepts is given in [40-41].

2.8.3. Dynamics

Finite-size effects in critical dynamics and in some nonequilibrium systems have been investigated recently [42]. Results were also obtained on finite-size effects on nucleation processes [43].

2.8.4. Random Systems

Finite-size scaling analysis of numerical simulation results for random systems, such as spin glasses or random-field models, has new interesting aspects associated with the use of two averages, one over randomness and the usual configurational ensemble average, as well as slow equilibration effects. These topics are reviewed in Young's article in this volume.

3. CRITICAL-POINT SCALING: SURVEY OF RESULTS

3.1. Definitions and notation

In this section we review recent numerical and analytical results for selected $2d$ and $3d$ models with an emphasis on scaling function universality and finite-size amplitudes. However, we first introduce notational conventions for thermodynamic and other quantities of interest.

3.1.1. Thermodynamic Quantities

Relation (2.62) for the magnetization contains an inconvenient factor $k_B T$. It is customary to define the reduced field

$$h = \frac{H}{k_B T}, \quad (3.1)$$

so that

$$M = -\frac{\partial f}{\partial h}. \quad (3.2)$$

Similarly, we define the susceptibility,

$$\chi = \frac{\partial M}{\partial h}, \quad (3.3)$$

i.e., with an extra factor of $k_B T$ as compared to the usual thermodynamic definition $\frac{\partial M}{\partial H}$. Note that no claim is made that h is dimensionless. In fact, we do not pay much attention to the particular choice of units of various quantities, as long as it is consistent.

We also introduce nonlinear “magnetization”,

$$M^{(nl)} = \frac{\partial \chi}{\partial h} \quad , \quad (3.4)$$

and “susceptibility”,

$$\chi^{(nl)} = \frac{\partial M^{(nl)}}{\partial h} \quad . \quad (3.5)$$

For bulk amplitudes in the limit $t \rightarrow 0^\pm$, we denote

$$M(t, 0; \infty) \approx B_- |t|^\beta, \quad t \rightarrow 0^-, \quad (3.6)$$

$$\chi(t, 0; \infty) \approx \Gamma_\pm |t|^{-\gamma}, \quad t \rightarrow 0^\pm \quad , \quad (3.7)$$

$$M^{(nl)}(t, 0; \infty) \approx B_-^{(nl)} |t|^{-(\gamma+2\Delta)}, \quad t \rightarrow 0^- \quad , \quad (3.8)$$

$$\chi^{(nl)}(t, 0; \infty) \approx \Gamma_\pm^{(nl)} |t|^{-(\gamma+2\Delta)}, \quad t \rightarrow 0^\pm \quad . \quad (3.9)$$

3.1.2. Binder’s Cumulant Ratio

Binder [38] proposed to define the quantity

$$G(t; L) = - \left[\frac{\chi^{(nl)}}{L^d \chi^2} \right]_{H=0} \quad . \quad (3.10)$$

By differentiating (with respect to h) the finite-size scaling form (1.10) for f , we conclude that G scales according to

$$G(t; L) \approx \mathcal{G}\left(atL^{1/\nu}\right), \quad (3.11)$$

and $G(0; L)$ approaches a universal value, $\mathcal{G}(0)$, as $L \rightarrow \infty$. More precisely, we have

$$\mathcal{G}(\tau) = \left[(\partial^4 Y / \partial \omega^4) / (\partial^2 Y / \partial \omega^2)^2 \right]_{\omega=0}, \quad Y \equiv Y(\tau, \omega). \quad (3.12)$$

If we denote by Ψ the fluctuating order parameter density, *i.e.*, $\langle \Psi \rangle = M$, then for hypercubic or near-hypercubic samples of volume L^d , we have

$$G(t; L) = \frac{3\langle \Psi^2 \rangle^2 - \langle \Psi^4 \rangle}{\langle \Psi^2 \rangle^2}. \quad (3.13)$$

This formula suggests the term “cumulant ratio” for G . Such “fluctuation” relations usually can be written down only for fully finite systems. For example, for the cylindrical geometry $L^{d-1} \times \bar{L}$, we have

$$G(t; L, \bar{L}) = \frac{\bar{L}}{L} \frac{3\langle \Psi^2 \rangle^2 - \langle \Psi^4 \rangle}{\langle \Psi^2 \rangle^2}. \quad (3.14)$$

This quantity has a finite limit, which we denote $G(t; L)$, as $\bar{L} \rightarrow \infty$.

3.1.3. Types of Surfaces (Boundary Conditions)

Surface interactions may be characterized by J_{wall} , different from the bulk coupling J . As long as J_{wall}/J is not too large, the

surface critical behavior is driven by the bulk. This is called the ordinary (O) surface transition. The most familiar case is $J_{wall} = J$, *i.e.*, *free boundary conditions*. It is believed that a continuous field-theoretical description near T_c with the constraint that the order parameter vanishes at the wall, corresponds to the O -type surface transition.

When J_{wall}/J increases, the surface may actually order above T_c . However, at T_c , singularities still develop in surface properties. This is termed the extraordinary (E) transition. The borderline case is termed the special (Sp) surface transition. Finally, wall interactions may result in a positive (+) or negative (-) ordering field H_{wall} acting at the surface. This case is believed to be universal also with a continuous field-theoretical order parameter fixed at positive (+) or negative (-) value at the surface.

The above surface types are, strictly speaking, valid only for the short range Ising models in $3d$. In $2d$, only O and \pm surfaces are possible. For models other than Ising, different classifications of boundary conditions may be appropriate.

For the finite-size scaling description, only the surface type (O , E , Sp , +, -, *etc.*) is important. The finite-size scaling functions are different for various types of boundary conditions.

3.2. Results for Cumulant and Other Ratios

3.2.1. Binder's Cumulant Ratio at T_c

For *hypercubic Ising* models, the value of $\mathcal{G}(0)$ in (3.11) has

been estimated by MC [34,38,44-47], transfer matrix combined with MC [48], Wilson's [49] approximate RG [50], and ϵ -expansion [5] methods, mostly with *periodic* boundary conditions. For periodic systems, estimates in $2d$ [44,48] suggest values in the range 1.830-1.835; estimates in $3d$ [5,38,46-47] suggest $\mathcal{G}(0) = 1.2\text{-}1.4$. Numerical studies in $5d$ [34] suggest the value $\mathcal{G}(0) \sim 1.0$, barely consistent with the mean-field result $0.81156\dots$ [5]. Further results for *free* boundary conditions can be found in [38].

Calculations for finite systems which are subblocks of larger systems (this can be regarded as another type of boundary conditions) yield values in the range 1.53-1.74 in $2d$ [38,50] and ~ 0.6 to ~ 0.9 in $3d$ [38,45,50]. Results in $4d$ [38], suggesting $\mathcal{G}(0) \sim 0$, should be considered preliminary, especially in view of the fact that the modified scaling relation (2.57), which in turn suggests

$$G(t; L) \approx \mathcal{G}\left(\bar{a}tL^{d/2}\right), \quad (3.15)$$

has been established only for $d > 4$, while the behavior of $G(t; L)$ in $4d$ has not been investigated theoretically.

For hypercubic, periodic n -vector models with $n > 1$, the only available result [5] is the $O(\epsilon)$ expansion in powers of $\sqrt{\epsilon}$, which is rather cumbersome and is not reproduced here. Note also that higher-order cumulant ratios, involving $\langle \Psi^6 \rangle$, *etc.*, have been considered [5,38,51], but no definitive numerical results are available. Finally, we quote an estimate $\mathcal{G}(0) = 1.934 \pm 0.001$ for $2d$ percolation [52].

Turning now to the *periodic cylinder* geometry, $L^{d-1} \times \infty$, we first quote the $3d$ results for the Ising model, $\mathcal{G}(0) \sim 3$, and for percolation, 5.0 ± 0.2 , obtained by the transfer matrix MC method [52]. More results are available in $2d$. Conformal invariance predictions [53-54] for the $2d$ Ising correlation functions on the $L \times \infty$ strip, have been integrated [48] to yield

$$\mathcal{G}(0) = 7.38132 \pm 0.00006, \quad (3.16)$$

which has been confirmed by transfer matrix [48] and transfer matrix MC [52] estimates to about 1%. Numerical results are also available for $2d$ percolation, 9.90 ± 0.06 [52], and 3-state Potts model, 2.49 ± 0.09 [55]. For $2d$ models with small exponent η , a general conformal invariance prediction [7] is

$$\mathcal{G}(0) \simeq \frac{6}{\pi\eta}, \quad \text{for } \eta \ll 1. \quad (3.17)$$

For disordered $2d$ Ising and 3-state Potts models, the estimates ~ 7.38 and 4.5 ± 0.9 , respectively, [55] illustrate a clear change of the universal $\mathcal{G}(0)$ value as compared to “pure” models, only in the 3-state Potts case ($\alpha = \frac{1}{3} > 0$), but not in the Ising case [compare (3.16)] which is borderline ($\alpha = 0$) according to the Harris [56] criterion.

3.2.2. Cumulant Scaling Asymptotics

The scaling function $\mathcal{G}(\tau)$ in (3.11) is universal for any value of τ . Numerical evaluation of this function for $\tau \neq 0$ (e.g., [34,38])

has been limited, as compared to the results at $\tau = 0$ described above. However, one can derive the asymptotic behavior in the limits $\tau \rightarrow \pm\infty$. For $\tau \rightarrow +\infty$, one can show [38,51], by considering large- τ behavior of the finite-size scaling functions, that

$$\mathcal{G}(\tau \rightarrow +\infty) \approx -\Gamma_+^{(nl)} \Gamma_+^{-2} (\tau/a)^{\alpha-2}. \quad (3.18)$$

This result applies for hypercubic systems, for all n , although the corrections to the power law decay (3.18), which are probably exponentially small in τ for periodic boundary conditions, have been considered carefully only for $n = 1$ [51]. Note that the coefficient of $1/\tau^{2-\alpha}$ is generally positive.

The detailed asymptotic prediction for $\tau \rightarrow -\infty$ has been derived [51] for periodic hypercubes, for $n = 1$ only, based on certain results on finite-size rounding of Ising first-order transitions [4], see Sect. 5. With

$$\bar{\tau} \equiv -\tau/a, \quad (3.19)$$

we have

$$\mathcal{G}(\tau \rightarrow -\infty) \approx \frac{2B_-^4 \bar{\tau}^{3(2-\alpha)} - 4B_- B_-^{(nl)} \bar{\tau}^{2-\alpha} - \Gamma_-^{(nl)}}{\bar{\tau}^{2-\alpha} (B_-^2 \bar{\tau}^{2-\alpha} + \Gamma_-)^2}, \quad (3.20)$$

where again the corrections are believed to be exponentially small in $\bar{\tau}$. Note that $\mathcal{G}(-\infty) = 2$.

3.2.3. High-Order Free Energy Derivative Ratios at T_c

Due to the $H \leftrightarrow -H$ symmetry which is not spontaneously broken even below T_c in fully finite, or effectively $1d$ cylindrically shaped systems, odd h -derivatives of the free energy vanish when $H \rightarrow 0^\pm$, as long as $L < \infty$. However, one can introduce [57] functions

$$f_{(+)}(T, H; L) = f_{(-)}(T, -H; L), \quad (3.21)$$

calculated from the two largest Ising model transfer matrix eigenvalues in the periodic cylinder geometry, which break the $H \leftrightarrow -H$ symmetry for $L < \infty$, and also approximate the $T < T_c$ “spontaneous” values of the free energy derivatives at $H = 0$, for $L < \infty$: see also Sect. 5.

Let $Y_{(+)}(\tau, \omega)$ denote the finite-size scaling function for $f_{(+)}$. The function $Y_{(+)}(0, \omega)$ was studied in [4], for the square and triangular lattice Ising model strips $L \times \infty$, with L up to ten lattice spacings. Universal ratios

$$\left. \frac{[\partial^{k+1} Y_{(+)}(\tau, \omega)/\partial \omega^{k+1}] [\partial^{k-1} Y_{(+)}(\tau, \omega)/\partial \omega^{k-1}]}{[\partial^k Y_{(+)}(\tau, \omega)/\partial \omega^k]^2} \right|_{\tau, \omega=0} \quad (3.22)$$

were estimated for $k = 2, 3, 4, 5, 6$. The values for two lattices agree to within 4% for $k = 2, 6$, but to better than 1% for $k = 3, 4, 5$.

3.3. Free Energy and Correlation Length Scaling

Most of this subsection is devoted to a survey of numerical and analytical tests of the finite-size scaling relations (1.10)-(1.11) and (1.13)-(1.14) in those geometries where these relations apply (see Sect. 2). Results for free-boundary-condition cubes and squares, where additional logarithmic scaling contributions enter (Sect. 2.5), are presented in the last Sect. 3.3.8.

3.3.1. Spherical Model Results

The $H = 0$ free energy scaling relation (1.10) was checked for spherical models in several geometries, with continuously varying $2 < d < 4$, and also with formally continuous number of finite dimensions, d^* , *i.e.*, for sample shapes $L_1 \times L_2 \times \dots \times L_{d^*} \times \infty \times \dots \times \infty$. Rather complicated implicit equations for $Y(\tau, 0)$ were derived, confirming its universality, for systems with periodic [58] and antiperiodic [59] boundary conditions, as well as for a class of Bose gas models [60] which are in the same universality class. Some scaling predictions for $d > 4$, see (2.52)-(2.53), *etc.*, were tested by spherical model calculations, reported in [61].

Tests of the correlation length scaling have been focussed mainly on calculating the universal amplitude $X(0, 0)$ in (1.14), in the periodic cylinder geometry $L^{d-1} \times \infty$, with varying $2 < d < 4$. Large- n limit results (equivalent to the spherical model [62]) are $X(0, 0) \simeq 0.6614$ in $3d$ [14] and

$$X(0,0) \approx (4\pi^2\epsilon)^{-1/3} \quad (3.23)$$

for small $\epsilon = 4 - d$ [14],

$$X(0,0) \approx (\pi\bar{\epsilon})^{-1} \quad (3.24)$$

for small $\bar{\epsilon} = d - 2$ [63], etc. Results for antiperiodic boundary conditions are also available [64], and furthermore it is known [64] that the appropriate amplitudes for the energy-energy correlation length are twice the spin-spin amplitudes, for both periodic and antiperiodic boundary conditions. Detailed results for correlation length scaling for $d \geq 4$ were also obtained, only at T_c , see, e.g., [14]. Specifically, the logarithmically modified L -dependence,

$$\xi(0,0;L) \approx L \left[(4\pi^2)^{-1} \ln L \right]^{1/3}, \quad (d=4), \quad (3.25)$$

is among the very few explicit results available in $d = 4$ [14].

3.3.2. ϵ -Expansion Results

As mentioned in Sect. 2, ϵ -expansions for finite-size systems [5,16-18,30-32,39] generally confirm the phenomenological scaling predictions. However, explicit results are difficult to derive. For periodic cylinders, an $O(\epsilon)$ closed-form expression is available [5] for $X(0,0)$, extending (3.23) to all $n \leq \infty$.

3.3.3. Numerical Estimates of 3d Amplitudes

For *periodic cubes*, L^3 , MC estimates are available for the SC and BCC Ising models [65], suggesting $Y(0, 0) = -(0.64\text{--}0.69)$. For both periodic and antiperiodic Ising cylinders, $L^2 \times \infty$, in the Hamiltonian (anisotropic) limit, numerical results are available [66–69] supporting the universality of $Y(0, 0)$ and $X(0, 0)$, both spin-spin and energy-energy.

For 3d slabs, $L \times \infty^2$, with various boundary conditions at each of the two surfaces, the singular part of the free energy scales according to (1.10) because this nonperiodic geometry has no corners (see Sect. 2.5). However, $Y(0, 0)$ depends on both boundary conditions which, as described in Sect. 3.1.3, can be any pair selected from $O, E, Sp, +, -$.

Results for 3d Ising amplitudes $Y(0, 0)$ have been summarized in [70]. Their Migdal-Kadanoff real-space RG values are 0.279, $\sim 0^-$, 0.017, 0.051, 0.019, 0.017, and -0.015 , for walls $+-$, $++$, $Sp+$, $O+$, $SpSp$, OSp , OO , respectively. Note also obvious symmetries $Y_{O+} = Y_{O-}$, etc. The OO value in the range $-(0.10\text{--}0.02)$ is also suggested by ϵ -expansion results [30]. For type E walls, it has been conjectured [70] that

$$Y_{AE}(0, 0) = Y_{A+}(0, 0), \quad (3.26)$$

for $A = O, E, Sp, +, -$. There are also certain mean-field relations among amplitudes which may hold approximately in 3d, see [70]. Numerical results for $n > 1$ are limited to some estimates for the

case $n = 2$: see [71] for details.

Numerical MC results are also available [33] for surface free energy amplitudes: see discussion leading to relation (2.51), in Sect. 2.6. Universality of $Y^{(\text{surface})}(0)$ has been checked [33] for various aspect ratios of 3d boxes (Sect. 2.6), for SC and BCC Ising models.

3.3.4. Conformal Invariance in 2d

Conformal invariance (*e.g.*, [7, 72]) yields exact values of critical exponents and universal finite-size amplitudes at T_c , for a large number of undirected 2d models. We do not review this rapidly growing field here. However, in the following subsections (Sect. 3.3.5-3.3.8), when surveying results for 2d amplitudes, we quote various conformal invariance predictions. We limit our discussion to the most familiar models (Ising, Potts, *etc.*).

3.3.5. Correlation Lengths for $L \times \infty$ Strips

For the spin-spin correlation length of the exponential decay of correlations along $L \times \infty$ strips in 2d, we have [53] conformal invariance results

$$X(0,0) = \frac{1}{\pi\eta}, \quad \text{and} \quad X(0,0) = \frac{2}{\pi\eta_{||}}, \quad (3.27)$$

for *periodic* and *free* boundary conditions, respectively, where η and $\eta_{||}$ are the standard bulk and surface exponents. Results for other correlations (*e.g.*, energy-energy) are similar, with appropriate exponents. For example, for the Ising model $\eta = \eta_{\text{spin-spin}} = \frac{1}{4}$, while

$$\eta_{\text{energy-energy}} = 2.$$

Another line of modification is to fix boundary conditions other than free (type O): (3.27) then applies with modified $\eta_{||}$. For example, we have $\eta_{||} = \eta_{||}(OO) = 1$, but $\eta_{||}(++) = \eta_{||}(--) = 4$, for the Ising model. These results have been derived and reviewed in [7,73]. Various exponents entering (3.27) and generalizations, have been determined exactly for many $2d$ models, including n -vector models with $|n| \leq 2$, and q -state Potts models with $0 \leq q \leq 4$, see [7,73]. For some cases (Ising, 3,4-state Potts), results have been derived also for antiperiodic and mixed boundary conditions [73].

More general tests of the finite-size scaling relation (1.11) have been mostly limited to the $2d$ Ising model in zero field. Thus $X(\tau, 0)$ has been calculated for periodic, antiperiodic, free, fixed, and some mixed-type boundary conditions [67-69,74-75]. Numerical transfer-matrix tests of universality of quantities derivable from $X(\tau, \omega)$ were also reported [75] for the 3-state Potts, spin- $\frac{1}{2}$ and spin-1 Ising, and some other models.

3.3.6. Second-Moment Correlation Length Amplitudes in $2d$

For a correlation length defined via the second moment of the correlation function of $L \times \infty$ strips, instead of the exponential decay definition (as in Sect. 3.3.5), the conformal invariance expression replacing (3.27) (assuming *periodic* boundary conditions), is [76]

$$X(0, 0) = \frac{1}{4\pi} \sqrt{2\psi' \left(\frac{\eta}{4} \right) - \frac{\pi^2}{\sin^2(\pi\eta/4)}} \quad , \quad (3.28)$$

where

$$\psi'(x) = \sum_{k=0}^{\infty} \frac{1}{(x+k)^2} \quad (3.29)$$

is the derivative of the standard digamma function $\psi(x)$. MC tests of this result for the self-avoiding walk model [76], for which $\eta = \frac{5}{24}$ and (3.29) yields $X(0,0) = 1.527\dots$, confirm the predicted value to about 2%, for strips up to 15 lattice spacings wide. Numerical MC results were also obtained [76] for strips with *free* boundary conditions, and compared with some approximate conformal invariance predictions (see [7,76]).

3.3.7. Tests of Free Energy Scaling in 2d

For *periodic* strips, $L \times \infty$, we have [77]

$$Y(0,0) = -\frac{\pi c}{6}, \quad (3.30)$$

where c is the conformal anomaly number. For example, $c = \frac{1}{2}$ for the 2d Ising universality class. For *free* or *fixed* (same on both sides of the strip) boundary conditions, we have [77]

$$Y(0,0) = -\frac{\pi c}{24}. \quad (3.31)$$

A point of caution is in order for the case of the 2d Ising model. When $\alpha = 0$, results like (3.30) refer to the “regular” scaling functions of the type $W(\tau)$ in (2.22), with logarithmic size dependence

separated out (and vanishing at T_c , since logarithmic terms are proportional to t^2), not to functions $\bar{W}_\pm(\tau)$, as in (2.21). Thus, $W(0) = -\pi/12$. For some models, conformal invariance results are also available for more complicated boundary conditions [73]. For instance, we have [73] $W(0)/\pi = \frac{1}{6}, \frac{23}{48}, \frac{1}{24}$, for Ising strips with antiperiodic, mixed $+-$, and mixed $O+$ (or $O-$) boundary conditions, respectively.

Numerical tests of the above predictions have been largely limited to systems with periodic boundary conditions and were carried out for several models, *e.g.*, $0 \leq q \leq 4$ Potts, *etc.* [67-69,75,77].

Results on the free energy scaling away from T_c are limited to the zero-field Ising model with various boundary conditions, in rectangle geometry $L_1 \times L_2$, see [13,78-79]. However, at T_c , results for $Y(0,0)$ are available for $0 \leq q \leq 4$ Potts model rectangles with several types of boundary conditions [80]. The expressions are rather complicated, involving θ -functions, *etc.* In some limits, explicit answers were given [78,80]. For example, for periodic Ising squares,

$$W(0) = -\ln \left(2^{1/4} + 2^{-1/2} \right) = -0.6399\dots . \quad (3.32)$$

3.3.8. Free-Energy Amplitudes for Systems with Corners

Thus far, the only numerical and analytical results testing predictions (2.33)-(2.34) were obtained at T_c , where the characteristic universal size dependence $yL^{-d} \ln L$ can be isolated ($d = 2, 3$). In $3d$, MC estimates

$$y = 0.009 \pm 0.005 \quad \text{and} \quad 0.012 \pm 0.003 \quad (3.33)$$

were reported [29] for, respectively, the SC and BCC-lattice Ising cubes, L^3 , with free boundary conditions. These studies also yielded universal surface and edge free energy amplitudes, see [29].

In $2d$, conformal invariance predictions are available for y [28], in rather general geometries with curved boundaries, corners, and in curved space. The amplitude y is then a global property [28]. We only survey the case of flat boundaries where we can attribute $y^{(\text{corner})}$ to each corner, see (2.35). With same (free or fixed) boundary conditions all over the polygon, each corner “geometry” is fully specified by the opening angle δ , and we have [28] the remarkable result

$$y^{(\text{corner})} = \frac{c\delta}{24\pi} \left[1 - (\pi/\delta)^2 \right]. \quad (3.34)$$

4. SIZE EFFECTS ON INTERFACIAL PROPERTIES

4.1. Interfacial Free Energy Near Criticality

4.1.1. Periodic Interfaces

Similar to the surface free energy (Sect. 2.6), interfacial free energy for finite-size systems is defined by a difference in the free energies of two samples with different boundary conditions. Con-

sider for example $L^{d-1} \times \bar{L}$ Ising boxes with periodic boundary conditions in all $d-1$ dimensions L . A “floating” periodic interface of hyperarea L^{d-1} can be introduced by imposing antiperiodic or $+-$ boundary conditions along \bar{L} . The appropriate boxes with no interfaces are with periodic and $++$ (or $--$) boundary conditions along \bar{L} , respectively. Note that we have to use $++$ for $+-$ to avoid any excess surface free energy. The excess interfacial free energy is then defined per $k_B T$ and per unit area,

$$\sigma(t; L, \bar{L}) = \bar{L} [f_{+-}(t; L, \bar{L}) - f_{++}(t; L, \bar{L})]. \quad (4.1)$$

A similar difference can be defined for antiperiodic *vs.* periodic boundary conditions along \bar{L} . The resulting function $\sigma(t; L, \bar{L})$ depends on the boundary conditions and other geometrical features such as the aspect ratio \bar{L}/L . In the limit $L, \bar{L} \rightarrow \infty$ with fixed t , the quantity $\sigma(t; L, \bar{L})$ approaches the bulk surface tension

$$\sigma^{(b)}(t) = \sigma(t; \infty, \infty), \quad (4.2)$$

where $\sigma^{(b)}(t) = 0$ for $t \geq 0$, and

$$\sigma^{(b)}(t) \sim (-t)^\mu, \quad \text{for small } t < 0. \quad (4.3)$$

The finite-size free energy difference (4.1) can in principle be considered for any model, in nonzero field, *etc.* However, it is customary to restrict the consideration to discrete spin systems (*e.g.*, Ising, Potts) at the phase boundaries ($H = 0, t \leq 0$ for the Ising case) where phases coexist and are separated by sharp interfaces.

Thus, most of our discussion refers to the $H = 0$ Ising models. However, we keep general t . Indeed, the hyperuniversal scaling form [4,81]

$$\sigma(t; L, \bar{L}) \approx L^{1-d} \Sigma \left(atL^{1/\nu}; \bar{L}/L \right) \quad (4.4)$$

involves a scaling function which is, as usual, smooth (analytic) at $\tau = atL^{1/\nu} = 0$. Note that we have not used “singular part” in (4.4). Indeed, for periodic “floating” interfaces relation (4.1) suggests that all the “nonsingular” terms in the free energies cancel out.

4.1.2. Exact and Numerical Results for Periodic Interfaces

All the available data on interfacial finite-size properties near T_c is limited to $2d$ models. For the $2d$ Ising model, the function $\Sigma(\tau; \bar{L}/L)$ can be evaluated exactly [82] in the $+-$ geometry described in Sect. 4.1.1. For example,

$$\Sigma(0; 1) = 0.86837 \dots . \quad (4.5)$$

For the 3-state Potts model, with $+-$ replaced by fixing Potts variables at different values at two walls, a MC study [83] of the scaling relation (4.4) yields, *e.g.*,

$$\Sigma(0; 1) \simeq 2.1. \quad (4.6)$$

For the antiperiodic geometry (Sect. 4.1.1), results are available for $0 \leq q \leq 4$ Potts models at T_c [80] (consult [80] for the definition

of “antiperiodic” for $q \neq 2$). For Ising ($q = 2$) squares, we have [80]

$$\Sigma(0; 1) = \ln(1 + 2^{3/4}) \simeq 0.9865, \quad (4.7)$$

which, when compared with (4.5), illustrates dependence on boundary conditions.

Note that singling out the size L to “scale” (4.4) leads to a singular dependence on \bar{L}/L in the limit of a long strip $L \rightarrow \infty$. For instance in the Ising case [84], we have

$$\Sigma(0; z) \approx \frac{\pi}{4z}, \quad \text{as } z \rightarrow 0, \quad (4.8)$$

which simply means

$$\sigma(0; \infty, \bar{L}) \approx \pi/(4\bar{L}). \quad (4.9)$$

Obviously, one can redefine (4.4), scaled with \bar{L} or any other combination of L and \bar{L} .

4.1.3. Pinned Interfaces

One can define interfacial free energy in geometries with interfaces with pinned boundaries (pinned ends in $2d$). An Ising $L \times \bar{L}$ system in $2d$, with an interface inclined by an angle δ , is illustrated in Fig. 1. Let Z_δ denote the appropriate partition function, and Z_+ denote the partition function with all + boundary conditions. Then we have

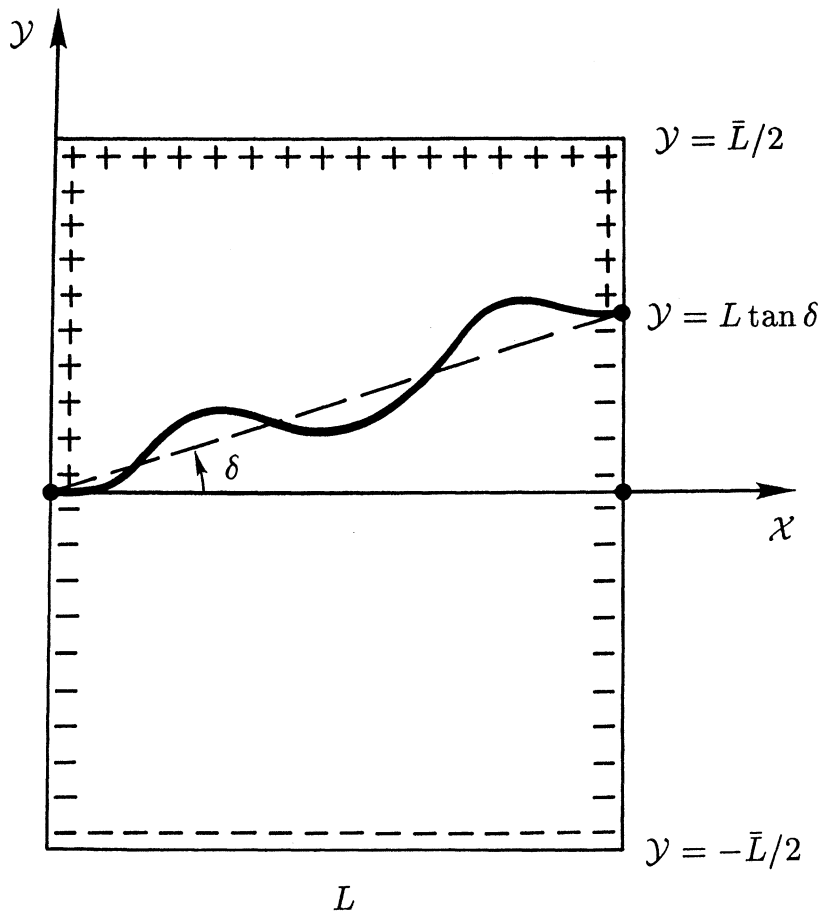


Figure 1: Pinned-end 2d interface inclined by an angle δ with respect to the \mathcal{X} -axis.

$$\sigma(t; L, \bar{L}; \delta) = -\frac{\cos \delta}{L} \ln \frac{Z_\delta}{Z_+}, \quad (4.10)$$

where $(L/\cos \delta)$ is the interfacial length (Fig. 1).

Quite generally, viewing interfacial free energy as a properly “normalized” free energy difference of two d -dimensional systems, we note that pinned-boundary interfaces have additional geometrical features of relative size $\sim L^{-2}, L^{-3}, \dots, L^{-d}$, per unit volume, as compared to the reference system with no interface. Thus, the non-singular background terms will not cancel out in these orders. When considered per unit area, we thus anticipate background terms of order $L^{-1}, L^{-2}, \dots, L^{-(d-1)}$, in σ , to play the role of similar terms in the free energy scaling. Specifically, the $L^{-(d-1)}$ contribution will “resonate” with the scaling part (in integer d) to yield universal terms $\sim L^{1-d} \ln L$. Thus, for nonperiodic interfaces of characteristic size L , one can propose [85] the equivalents of (2.33)-(2.34), with integer d ($d = 2, 3$),

$$\begin{aligned} \sigma(t; L) \approx & \frac{1}{L} \sigma_{ns}^{(1)}(t) + \dots + \frac{1}{L^{d-1}} \sigma_{ns}^{(d-1)}(t) \\ & + L^{1-d} \left[\tilde{\Sigma} \left(atL^{1/\nu} \right) + s \ln(L/l) \right]. \end{aligned} \quad (4.11)$$

Here s and $\tilde{\Sigma}(\tau)$ are universal, although they may depend on the geometries used to define $\sigma(t; L)$, *i.e.*, shape, boundary conditions, *etc.* Note that as for the free energy, the background terms of higher order and correction-to-scaling terms must be allowed for a fuller description.

4.1.4. Exact 2d Ising Results for Pinned Interfaces

For the 2d Ising geometry of Fig. 1 with $\bar{L} \rightarrow \infty$, the partition function ratio in (4.10) was calculated exactly for $t < 0$ [86] and recently analyzed in the limit $t \rightarrow 0^-$ [87]. For this 2d geometry, relation (4.11) is indeed confirmed. One finds [85,87]

$$s = 1, \quad (4.12)$$

and an explicit quadrature for $\tilde{\Sigma}(\tau \leq 0)$, as well as background terms of order $1/L$ [see (4.11)] and higher. Interestingly, $\tilde{\Sigma}(\tau)$, but not s , depends on the angle δ which is a geometrical feature here.

4.2. Interfacial Free Energy Below Criticality

In this subsection we consider finite-size free energy contributions due to Gaussian “capillary” interfacial fluctuations above the roughening temperature, which are a critical-type soft mode phenomenon. Thus, we take fixed $T_R < T < T_c$, where $T_R = 0$ in 2d, but $T_R > 0$ for 3d lattice models and, in fact, may depend on interface orientation. Since we are now considering behavior away from T_c , there is no critical part. However, capillary fluctuations contribute [88-89] a universal (geometry-dependent) term $vL^{1-d} \ln L$. Thus far, only integer d were studied; for an interface of a characteristic size L , we expect [88-89], in integer d ,

$$\begin{aligned} \sigma(t; L) &= \sigma(t; \infty) + \frac{1}{L} \sigma^{(1)}(t) + \frac{1}{L^2} \sigma^{(2)}(t) + \dots \\ &\quad + \frac{1}{L^{d-1}} \sigma^{(d-1)}(t) + \frac{v}{L^{d-1}} \ln\left(\frac{L}{l}\right) + o\left(\frac{1}{L^{d-1}}\right). \end{aligned} \tag{4.13}$$

The association of terms in (4.13) with geometrical characteristics is not straightforward. Indeed, for periodic interfaces, the contributions $\sigma^{(j)}(t)/L^j$ vanish identically for $j = 1, \dots, d - 2$, however, the logarithmic and $O(L^{1-d})$ terms are still present [89], which is a special feature of Gaussian models. One finds [89] that

$$v = 1 \tag{4.14}$$

for “floating” periodic interfaces in any integer d , provided L is defined so that L^{d-1} is the interface area. For other boundary conditions on the interface (pinned, “floating” with free ends, *etc.*), v is explicitly geometry-dependent [88-89].

Turning now to the $2d$ geometry of Fig. 1 for which detailed results are available [88] provided δ is small, and $\bar{L} \gg O(\sqrt{L})$, we note two interesting features. Firstly, size dependence no longer enters in ratios. The L -dependence is as in (4.13), with $d = 2$. However, finite- \bar{L} effects are of order $\exp(-\kappa \bar{L}^2/L)$, where $\kappa(T)$ is the surface stiffness coefficient [88]. Secondly, the universal amplitude v is a function of the inclination angle δ . For small δ , we have [85,88]

$$v = \frac{1}{2} - \frac{1}{4} \phi^2 + O(\phi^4). \tag{4.15}$$

Finally, we point out that for the geometry of Fig. 1 with $\bar{L} \rightarrow \infty$, exact $2d$ Ising model results [86] confirm the Gaussian model predictions.

4.3. Other Research Topics

The purpose of this subsection is to provide a brief reference to three additional research topics of growing interest, where both finite-size and interfacial properties are involved. No comprehensive review is attempted here. However, for completeness, we list recent literature. The subjects discussed are wetting transitions in finite-size geometries, fluctuations of unpinned interfaces including the relation of interfacial properties and the transfer matrix spectrum in cylindrical geometries, and recent MC results for step free energies near roughening transitions.

4.3.1. Size Effects on Wetting

Recently, several mostly mean-field type calculations were reported for $3d$ wetting transitions in the slab geometry $L \times \infty^2$ [90], on cylinders and spheres (in $3d$) [91], and also for the case where the interface itself is finite-size [92].

In $2d$, critical wetting in the strip geometry $L \times \infty$ was studied within the solid-on-solid model [93]. Another project [94] involved the exact $2d$ Ising solution for a finite-size rounded first-order interface unbinding transition in a $2d$ surface-plus-defect geometry, as well as some solid-on-solid model results. Generally, finite-size ef-

fects on wetting are a developing field, detailed survey of which is outside the scope of this review.

4.3.2. Fluctuating Interfaces in Cylindrical and Slab Geometries

In Sect. 4.2 we discussed size effects on the free energy of interfaces of finite extent in some or all $d - 1$ directions. In some other geometries, interfacial fluctuations are cut off due to finite size in the dimension transverse to the interface. For example, interfaces induced by $+-$ or antiperiodic boundary conditions in $2d$ strips ($L \times \infty$) or $3d$ slabs ($L \times \infty^2$) have infinite area (length in $2d$). Much progress has been made on fluctuations of line interfaces in $2d$, specifically, in the strip geometry, by numerical and exact $2d$ Ising [84,95] calculations and by solid-on-solid type modeling [93,96-98], equivalent to diffusion. Available results for slabs [98] are more limited. The issues investigated are how the free energy and correlations are modified by the transverse size. Specific results are, however, not reviewed here.

Recently, several authors considered transfer matrix spectrum and in particular, the leading spectral gap of Ising type models, with boundary conditions inducing an interface along a $2d$ strip [99]. For the $+-$ or antiperiodic boundary conditions, the correlation lengths defined by the transfer matrix spectral gaps have been related [97] to the bulk surface stiffness coefficient $\kappa(T)$. For example, the leading-gap correlation length is given by [97]

$$\xi(T < T_c; L) \approx \frac{2\kappa(T)L^2}{\pi^2} \quad \text{and} \quad \frac{2\kappa(T)L^2}{3\pi^2}, \quad (4.16)$$

for antiperiodic and $+-$ strips $L \times \infty$, with $L \rightarrow \infty$ at fixed $0 < T < T_c$. For $3d$ cylinders, $L \times \bar{L} \times \infty$, with antiperiodic or $+-$ boundary conditions along L , and with, *e.g.*, periodic boundary conditions along \bar{L} (so that the interface has width \bar{L}), the appropriate results have been derived for $T_R < T < T_c$ and separately, for $0 < T < T_R$. Above T_R , the spectrum is determined by $\kappa(T)$ and relations similar to (4.16) apply, with an extra factor of \bar{L} on the right hand sides. Below T_R , however, the spectrum is determined by the *step free energy*, $s(T)$, measured per $k_B T$ and per unit step length in a “terrace-shaped” rigid interface. The full expressions [97] require introducing further notation. Thus, we only quote that for large L ,

$$\xi(T < T_R; L, \bar{L}) \propto L^2 \sqrt{\bar{L}} e^{s(T)\bar{L}}, \quad (4.17)$$

without specifying the form of the coefficient (which is T -dependent). For free, instead of periodic, boundary conditions along \bar{L} , the factor $\sqrt{\bar{L}}$ should be omitted. The behavior at T_R has not been investigated, see also Sect. 4.3.3 below.

For cylindrical geometries, $L^{d-1} \times \infty$, with fully periodic, free, or other boundary conditions such that no *longitudinal* interfaces will be introduced, there occurs an interesting phenomenon of spontaneous generation of *transverse* interfaces [4,100] (for $T < T_c$ and $H = 0$). Their exponential separation defines a correlation length associated with the leading transfer matrix spectral gap,

$$\xi(T < T_c; L) \sim e^{\sigma(T)L^{d-1}}. \quad (4.18)$$

This form has been discussed recently [4-5,97,101] in connection with the finite size contributions to the difference

$$\tilde{\sigma}(T; L) - \sigma(T) \equiv \tilde{\sigma}(T; L) - \tilde{\sigma}(T; \infty), \quad (4.19)$$

where $\tilde{\sigma}$ is *defined* via

$$\xi(T; L) = \exp [\tilde{\sigma}(T; L)L^{d-1}]. \quad (4.20)$$

We will not review this topic further here (see [97,101] and Sect. 5.4.4 for details).

4.3.3. Step Free Energy Near Roughening Temperature

Recently, MC results were obtained for the step free energy of the cubic-shaped 3d Ising model with a stepped interface induced by periodic-antiperiodic-helical boundary conditions [102]. The results as $T \rightarrow T_R$ from below seem to be described [102] by a scaling form with L scaled by $[s(T)]^{-1}$. This single scaling variable description cannot, however, be fully satisfactory in general due to the Gaussian nature of the rough phase above T_R . In fact, finite-size behavior at the Kosterlitz-Thouless transitions in XY systems is also not fully understood theoretically, see, *e.g.*, recent accounts [103] and references quoted therein.

5. FIRST-ORDER TRANSITIONS

5.1. *Opening Remarks*

This section is devoted to finite-size effects at first-order transitions. We consider cubic or nearly cubic systems of volume $V = L^d$, as well as a crossover to long cylinders, $A \times L_{\parallel}$, of cross sectional area A and volume $V = AL_{\parallel}$, with, eventually, $L_{\parallel} \rightarrow \infty$. Most theoretical results available to date (see below) pertain to these geometries and furthermore, assume *periodic boundary conditions* in all finite dimensions.

It is generally believed that first-order transitions are controlled by the so-called *discontinuity fixed points* [104] of the RG transformations, which are characterized by having one or more RG eigenexponents equal the space dimensionality d . Results on finite-size rounding of first-order transitions can be generally cast in the appropriate RG scaling forms, and furthermore, one can discuss a crossover to critical point scaling near T_c : all these issues will be considered in the following subsections.

Reviews and comprehensive expository articles on finite-size effects at first-order transitions, both theory and numerical MC simulations, include references [4-6,105-107]. Certain numerical transfer matrix results are also available (see Sect. 5.4.5).

5.2. *Hypercubic Ising Models at the Phase Boundary*

Let us denote by M_0 the bulk spontaneous magnetization,

$$M_0 \equiv M(T < T_c, H \rightarrow 0^+; L = \infty). \quad (5.1)$$

In this subsection we consider *symmetric* first-order transitions exemplified by hypercubic or near-hypercubic ferromagnetic Ising models at fixed $T < T_c$, with the bulk magnetization approaching $\pm M_0$ as $H \rightarrow 0^\pm$. We assume periodic boundary conditions, so that the full $H \leftrightarrow -H$ symmetry is preserved in a finite system.

When such a system with $H \simeq 0$ is evolving in time under some model dynamics, it spends most of the time in the states with the fluctuating order parameter Ψ near $\pm M_0$, as is indeed observed in MC simulations [108]. The probability distribution for Ψ is then sharply peaked at $\pm M_0$ [38]. Thus, the “singular part” of the H -dependence of the free energy can be estimated [4,108-109] from the mimic partition function

$$e^{hM_0V} + e^{-hM_0V}, \quad (5.2)$$

where we used (3.1). For the magnetization, this yields

$$M_s(T, H; L) \approx M_0 \tanh(hM_0V), \quad (5.3)$$

which suggests that the transition (discontinuity $\pm M_0$ in the magnetization) is rounded on the scale

$$H_V = \frac{k_B T}{M_0 V} \sim \frac{1}{V}. \quad (5.4)$$

The susceptibility of finite system develops a sharp peak of width $\sim V^{-1}$ and area $2M_0$, representing the rounded delta-function $2M_0\delta(h)$. The shape of this peak is described by

$$\chi_s \approx M_0^2 V / \cosh^2(hM_0 V) . \quad (5.5)$$

Substantiation of the phenomenological arguments leading to (5.4)-(5.5) can be achieved in part [4] by considering sum rules like

$$\chi(T < T_c, H \equiv 0; L < \infty) \simeq M_0^2 V + \chi(T < T_c, H \rightarrow 0^+; L \equiv \infty) , \quad (5.6)$$

[compare (5.5) with $h = 0$], the validity of which relies on the fact that for finite Ising cubes, odd correlation functions vanish by symmetry ($H \leftrightarrow -H$) so that “connected” finite-size correlation functions are similar to bulk “full” correlation functions, see [4] for details. Better control of correction to, *e.g.*, (5.5), can be gained in the transfer matrix formulation [4] described in Sect. 5.4 below.

5.3. Cubic n -Vector Models in the Giant-Spin Approximation

5.3.1. Néel’s Mean-Field Theory of Superparamagnetism

We now extend our consideration to n -vector models with $n = 1, 2, 3, \dots$, still assuming periodic boundary conditions and near-cubic shapes. Néel [110] proposed a phenomenological mean-field type description of the development of the susceptibility contribution $\sim V$ in small single-domain magnetic particles, typically with

Heisenberg ($n = 3$) symmetry, see a review [111]. This phenomenon is termed *superparamagnetism*. In Néel's approach, the only fluctuations considered are rotations of the global order parameter $\vec{\Psi}$, which is an n -component vector for $n = 2, 3, 4, \dots$. Denoting unit vectors by overhats, as usual, the mimic partition function generalizing (5.2) to $n > 1$ is given by [107]

$$\int e^{hM_0 V(\hat{\Psi} \cdot \hat{H})} d^{n-1}\hat{\Psi}, \quad (5.7)$$

where the integration is over the $n - 1$ orientational (angular) coordinates of the vector $\vec{\Psi} = M_0 \hat{\Psi}$, with respect to the direction of the applied field $\vec{H} = H \hat{H}$. For the (longitudinal) magnetization, this yields

$$M_s \approx M_0 m(hM_0 V), \quad (5.8)$$

where the scaling function $m(x)$ for general n can be expressed [107] in terms of the standard Bessel functions as follows,

$$m(x) = I_{\frac{n}{2}}(x) / I_{\frac{n-2}{2}}(x). \quad (5.9)$$

For $n = 3$, $m(x)$ reduces [111] to the well known Langevin function,

$$m_{n=3} = \coth(x) - x^{-1}, \quad (5.10)$$

while for $n = 1$, relation (5.3) is formally reproduced. For the leading order longitudinal susceptibility peak at $H = 0$, we get

$$\chi_s(H=0) = M_0^2 V/n. \quad (5.11)$$

Corrections to the leading asymptotic results (5.8), (5.11), *etc.*, for $n = 2, 3, \dots$, turn out to be much more significant than for the case $n = 1$, due to spin-wave fluctuation contributions [107]. We will return to this issue in Sect. 5.5 below.

5.3.2. Giant-Spin Concept and Discontinuity

Fixed Point Scaling

The scaling combination in (5.8) can be rewritten as

$$hM_0V = \frac{M_0(T)H}{k_B T} L^d, \quad (5.12)$$

where all the T -dependence has been made explicit. As $T \rightarrow 0$, $M_0(T)$ approaches a constant value, so that the scaling combination involves a *linear scaling field* h , at the discontinuity fixed point at $H, T = 0$, with eigenexponent $\lambda_h^{(\text{discontinuity})} = d$, as anticipated [104]. Furthermore, it is natural to conjecture that the full T -dependent scaling field is $M_0(T)h$, where T enters as an irrelevant variable which in turn has negative eigenexponent $\lambda_T^{(\text{discontinuity})} = 1 - d$ or $2 - d$, for $n = 1$ and $n > 1$, respectively.

When taken seriously, this RG scaling interpretation can be used to calculate the scaling functions like $m(x)$ in (5.8), see [112]. Indeed, let l denote a microscopic lattice spacing, and iterate the RG transformation L/l times to obtain

$$h' = h(L/l)^d, \quad T' = T(l/L)^{d-d_0} \quad , \quad (5.13)$$

where $d_0 = 1$ for $n = 1$, $d_0 = 2$ for $n = 2, 3, \dots$. Thus, we obtained one spin with a “giant” magnetic coupling $\sim hL^d$, at a very low temperature $\sim TL^{d_0-d}$. By solving for the free energy of this “giant” spin, and using the standard RG free energy recursion

$$f_s(T, h; L) \approx (L/l)^{-d} f_s(T', h'; 1), \quad (5.14)$$

one can actually obtain information on the form of the scaling functions. In the cubic geometry, this method yields, *e.g.*, the result (5.9). Applications to cylindrical geometries [112] sometimes run into difficulties [4] associated with dangerous irrelevant variables, see Sect. 5.4.4 below.

5.3.3. Upper Critical Dimension for First-Order Transitions

The fact that RG iteration down to a single “giant” spin, and Néel’s mean-field theory which also, in a sense, assumes a rotating “giant” overall spin variable $\vec{\Psi}$, with $|\vec{\Psi}| = M_0$, both give the same results, at least in the leading order, suggests that first-order transitions are always technically above their upper critical dimension d_0 . The dimensionality d_0 is also the lower critical dimension for the critical point at $T_c > 0$. As mentioned, $d_0 = 1$ for Ising models ($n = 1$), and $d_0 = 2$ for n -vector models with $n = 2, 3, 4, \dots, \infty$. Exact calculations [113] for the long-range spherical models ($n = \infty$) for which d_0 varies continuously ($0 < d_0 < 2$) confirm this observation.

5.4. Crossover to Cylindrical Geometry: Ising Case

5.4.1. Longitudinal Correlation Length

For Ising models in the cylindrical geometry $A \times L_{\parallel}$, with periodic boundary conditions, it is useful to consider the transfer matrix evaluation of the partition function. If the transfer matrix \mathcal{T} adds up a slice of size $A \times l$, where l is of the order of lattice spacing, then the partition function is given by $\text{Tr}(\mathcal{T}^{L_{\parallel}/l})$. In terms of the ordered set of eigenvalues of \mathcal{T} ,

$$\Lambda_0 > \Lambda_1 \geq \Lambda_2 \geq \dots, \quad (5.15)$$

we have for the partition function,

$$\Lambda_0^{L_{\parallel}/l} + \Lambda_1^{L_{\parallel}/l} + \dots. \quad (5.16)$$

The free energy of the infinite cylinder, $A \times \infty$, is given by f_0 , where

$$f_j \equiv -\frac{1}{lA} \ln \Lambda_j, \quad (j = 0, 1, \dots), \quad (5.17)$$

denote the so-called free energy levels [57]. One can also introduce correlation lengths associated with the transfer matrix spectral gaps,

$$\xi_j \equiv l / [\ln (\Lambda_0 / \Lambda_j)], \quad (j = 1, 2, \dots). \quad (5.18)$$

For sufficiently long cylinders, one can no longer argue that the first order transition will be rounded according to (5.3) on the

scale H_V defined in (5.4). Indeed, when $L_{\parallel} \rightarrow \infty$, the total volume V diverges and so $H_V \rightarrow 0$. However, the transition must remain rounded in a one-dimensional cylinder. One then argues [4] that (5.3) is essentially a single-domain result. On the other hand, as mentioned in Sect. 4.3.2, long cylinders in zero field spontaneously form \pm domains of length [4,100] $\sim e^{\sigma A}$, associated with entropy gain [114]. This longest length scale ξ_{\parallel} in the $H = 0$ cylinder, describing the persistence of the order parameter values $+M_0$ or $-M_0$, must correspond to ξ_1 ,

$$\xi_{\parallel}(T; L) = \xi_1(T, H=0; L), \quad (5.19)$$

as is indeed confirmed by exact $2d$ Ising results [84] and other general considerations [4,100].

For the rounded first-order transition, one then anticipates that

$$M_s(T, H; L) \approx M_0 \tilde{m}(hM_0 V, L_{\parallel}/\xi_{\parallel}), \quad (5.20)$$

with

$$\tilde{m}(x, z \rightarrow 0) = m(x), \quad \text{for } L_{\parallel} \ll \xi_{\parallel}, \quad (5.21)$$

$$\tilde{m}(x, z \rightarrow \infty) = \bar{m}(x/z), \quad \text{for } L_{\parallel} \gg \xi_{\parallel}. \quad (5.22)$$

The correlation length ξ_{\parallel} is generally described by relations (4.18)-(4.20). We will return to its precise form in Sect. 5.4.4 below.

For the moment, the important feature is its exponential leading-order L -dependence, (4.18), which has been confirmed by exact $2d$ Ising results [84,100], and by numerical transfer matrix studies in $3d$ [115]. Note that for cylinders it is convenient to use the convention $A = L^{d-1}$ (Sect. 4), which should not be confused with $V = L^d$ used in subsections on cubes.

5.4.2. Calculation of the Scaling Functions

Before considering the implications of the scaling relation (5.20), it is helpful to outline calculations [4] yielding the exact result

$$\tilde{m}(x, z) = \frac{x}{\sqrt{x^2 + \frac{1}{4}z^2}} \tanh \sqrt{x^2 + \frac{1}{4}z^2} \quad , \quad (5.23)$$

which satisfies (5.21) and also gives [see (5.22)]

$$\bar{m}(\bar{x}) = \frac{\bar{x}}{\sqrt{\bar{x}^2 + \frac{1}{4}}} \quad , \quad (\bar{x} = x/z). \quad (5.24)$$

The theory leading to these explicit Ising model results is rather complicated [4,116]. Only the main steps will be presented here. First, we note that the two largest eigenvalues of the transfer matrix are asymptotically degenerate at $H = 0$ (for $T < T_c$), as is implied by the general relation

$$f_j - f_0 = (\xi_j A)^{-1}. \quad (5.25)$$

Indeed, for $j = 1$ the free energy values are split $\sim e^{-\sigma A}$. However,

this pair is isolated from the rest of the spectrum because the next gap, $f_2 - f_0$, defines the bulk correlation length $\xi^{(b)}$ which is finite at $H = 0$. Thus, $f_2 - f_0 \sim 1/A$. It turns out [4] that the two lowest free energies are well separated from the rest of the spectrum for

$$|H| < H_V \left(L_{\parallel} / \xi^{(b)} \right) \sim \frac{1}{A}, \quad (5.26)$$

compare (5.4).

The range (5.26) is wider than the finite-size rounding, both for $L_{\parallel} = O(L)$ and for $L_{\parallel} \rightarrow \infty$ (see below). One can show [4] that in this regime the mimic partition function describing the rounded transition is given by (5.16) with only the first two terms kept. The next step is to use the two-level model [57] description of the near degeneracy of f_1 and f_0 at $H = 0$. This allows a representation of f_0 and f_1 in terms of the *bulk* quantities, and ξ_{\parallel} , by using the concept of the single-phase free energy functions $f_{(\pm)}$, mentioned in Sect. 3.2.3, see (3.21). We only present the final expressions valid up to corrections of order H^3 and $e^{-L/\xi^{(b)}}$ (for periodic boundary conditions). Higher orders in h can be also evaluated, see [4,51] for details. We have

$$f_0 \approx f^{(b)} \mp \sqrt{M_0^2 h^2 + \frac{1}{4A^2 \xi_{\parallel}^2}} - \frac{1}{2} \chi^{(b)} h^2, \quad (5.27)$$

where (b) denotes evaluation in the bulk limit, with $h \rightarrow 0^+$ *after* setting $A, L_{\parallel} = \infty$. Finally, the expressions (5.27) are substituted in the mimic partition function (5.16), with (5.17).

The transfer matrix approach yields the leading-order scaling results for cubes, cylinders, and in the crossover regime $L_{\parallel} \simeq \xi_{\parallel}$. Thus, (5.23) is obtained from the leading free-energy expression [4]

$$f_s \approx -\frac{1}{V} \ln \left[2 \cosh \left(V \sqrt{M_0^2 h^2 + \frac{1}{4A^2 \xi_{\parallel}^2}} \right) \right], \quad (5.28)$$

where the size dependence enters not only via V, A , but also ξ_{\parallel} . Furthermore, as mentioned, control of correction terms is possible, although derivation of explicit results is rather cumbersome [51]. For illustrations, we mention the leading order correction to the “cubic” result (5.5),

$$\chi_s \approx \frac{M_0^2 V}{\cosh^2(h M_0 V)} + \chi^{(b)} \quad . \quad (5.29)$$

This relation extends the sum rule (5.6) to fields $|H| \leq O(H_V)$.

5.4.3. Cylindrical Limit Scaling

In the limit $L_{\parallel} \rightarrow \infty$, obtained for $L_{\parallel} \gg \xi_{\parallel} \sim e^{\sigma A}$, relations (5.20) with (5.22) and (5.24) should be used. One has

$$M_s \approx M_0 \bar{m}(h M_0 A \xi_{\parallel}), \quad (5.30)$$

so that the scaling combination involves the “correlated” volume $A \xi_{\parallel}$ instead of the total volume AL_{\parallel} . For the susceptibility peak, of area $2M_0$, we get

$$\chi_s \approx \frac{M_0^2 A \xi_{\parallel}}{4 \left[(h M_0 A \xi_{\parallel})^2 + \frac{1}{4} \right]^{3/2}}, \quad (5.31)$$

which is exponentially large (in A) at $h = 0$, where we have $\chi_s(h=0) \approx 2M_0^2 \xi_{\parallel} A$.

5.4.4. Size Dependence of ξ_{\parallel} and RG Scaling

As already alluded to in the discussion of relations (4.18)-(4.20), the cross-section size (and shape, *etc.*, or what we have generally called *geometry*, in Sect. 1-4) dependence of the quantity $\tilde{\sigma}(T; L)$ is of interest for several reasons [97,101]. Its general pattern (at least, for rough interfaces) should be similar to that of the Gaussian prediction (4.13). We will denote coefficients in such a relation for $\tilde{\sigma}$, by $\tilde{\sigma}^{(j)}(t)$ and \tilde{v} , compare (4.13).

Exact results for periodic [4], free [99,117], and some other [99] boundary conditions are available for 2d strips $L \times \infty$. The form (4.13) then applies, with $\tilde{\sigma}^{(1)}$ and \tilde{v} terms present in 2d. For the universal amplitude \tilde{v} , one finds

$$\tilde{v}_{\text{periodic},2d} = \frac{1}{2}, \quad \tilde{v}_{\text{free},2d} = 0. \quad (5.32)$$

However, the appropriate single-interface Gaussian model results (Sect. 4.2) were [89]

$$v_{\text{periodic}} = 1, \quad v_{\text{free},2d} = \frac{1}{2}. \quad (5.33)$$

It has been suggested that the difference $v - \tilde{v}$ is due to fluctuations of the dilute gas of interfaces [5,101,118]. This effect warrants further study.

The size dependence of $\tilde{\sigma}(T; L)$ complicates identification of (5.20) or (5.30) as RG scaling results. Indeed, in RG scaling we expect dependence on the *relevant* scaling combination hM_0V , already identified from the results for cubes. Shape ratio dependence is also possible, and allows us to isolate the L_{\parallel} dependence in (5.20),

$$L_{\parallel}/\xi_{\parallel} = (L_{\parallel}/L)(L/\xi_{\parallel}). \quad (5.34)$$

The remaining scaling variable is conveniently rewritten as

$$\frac{L}{\xi_{\parallel}} = e^{-\bar{\sigma}L^{d-1}}, \quad (5.35)$$

where

$$\bar{\sigma}(T; L) = \tilde{\sigma}(T; L) - L^{1-d} \ln L. \quad (5.36)$$

Since we define the interfacial free energies *per* $k_B T$, we have $\sigma(T) \sim T^{-1}$ as $T \rightarrow 0$. Thus, in the leading order in L , as $L \rightarrow \infty$, the scaling combination L/ξ_{\parallel} indeed depends on the leading irrelevant variable $\sim T$ at the discontinuity fixed point. The first-order transition scaling functions in the cylindrical limit $L_{\parallel} \gg \xi_{\parallel}$, and also for $L_{\parallel} = O(\xi_{\parallel})$ [relations (5.30) and (5.20)] are highly singular in their TL^{1-d} dependence, so that the irrelevant variable is dangerous.

The interpretation of the subleading L -dependence of the product $\bar{\sigma}^{-1}L^{1-d}$ is, however, less clear. Indeed, if we identify $\bar{\sigma}^{-1}$ as the full nonlinear irrelevant RG scaling field with eigenexponent $\lambda_T = 1 - d$, then it has explicit L -dependence. In the critical-point finite size scaling (Sect. 2) it has been emphasized that the scaling fields g_t, g_H, g_u [see (2.6)-(2.7), *etc.*] do not acquire L -dependence for $L < \infty$, and L enters as a “macroscopic” length. The origin of the breakdown of this observation at the Ising discontinuity fixed points is not clear. Ambiguities noted in [4], with the RG rescaling [112] of Ising cylinders down to $1d$ giant-spin chains, are also related to the importance of the L -dependent corrections to the irrelevant-variable scaling combination $\sim TL^{1-d}$.

5.4.5. Exact and Numerical Tests of Scaling for Ising Cylinders and Cubes

Exact calculations for finite-size rounded Ising first-order transitions have been reported for two models. First, studies of the infinite-range Ising model, which is usually used as a prototype model of mean-field critical points, yield results [4] on the phase boundary which in the leading order are consistent with the periodic cube predictions (5.3), *etc.* However, the pattern of corrections is generally different, see [4] for details. The other exact calculation is for the first-order *wetting transition* [94] in a certain $2d$ Ising geometry, mentioned in Sect. 4.3.1. In this case the mechanism of the rounding is similar to cylinders and follows the pattern of the two-level free-energy model.

Numerical transfer-matrix tests of the rounded magnetization scaling in $2d$ Ising-type model *strips* were reported in [119]. MC tests were also reported, for *square* Ising-model systems [105-106,108], including detection of the correction term in (5.29).

5.5. Spin-Wave Effects for $n = 2, 3, \dots, \infty$

5.5.1. Cylinder-Limit Scaling

Instead of breaking into \pm domains, the vector-spin models in cylindrical geometries have their order parameter slowly rotate. This random drift of the order parameter orientation, which may also be viewed as an ensemble of diffuse Bloch walls, or $\vec{k}_\perp = 0$, small- k_\parallel spin waves, leads to the absence of ferromagnetic n -vector ordering in $1d$. Analysis of this phenomenon within an effective longest-mode transfer matrix formulation was carried out in [107,120]. We do not review here this rather complicated formalism, but only summarize some results.

For the zero-field correlation length defining the persistence distance of the order parameter orientation, one finds [107,121],

$$\xi_\parallel(T; L) \approx \frac{2\Upsilon(T)A}{(n-1)k_B T} . \quad (5.37)$$

Here $\Upsilon(T)$ is the helicity modulus which some readers may have encountered in the form of the so-called spin-wave stiffness coefficient,

$$\rho_s \equiv \Upsilon(T)/k_B T . \quad (5.38)$$

The transfer matrix formulation [107] with nonzero applied field was used to establish the validity of the scaling description (5.20)-(5.22), for $|H| \leq O(H_V)$, with $m(x)$ in (5.21) given by (5.9). Exact closed form expressions for \tilde{m} and \bar{m} are not known. However, $\bar{m}(\bar{x})$ can be obtained from the ground state of a certain quantum-mechanical Hamiltonian [107]. Thus, numerical and approximate analytical results for $\bar{m}(\bar{x})$ can be derived, although results available to date are very limited.

By considering the scaling combination $L_{\parallel}/\xi_{\parallel}$, similar to the Ising case, we can conclude that the irrelevant RG field $\sim T$, with eigenexponent $\lambda_T = 2 - d$, is given by

$$\frac{(n-1)k_B T}{\Upsilon(T)} . \quad (5.39)$$

Since this expression is not dependent on L , the ambiguities of the Ising case are not present here. Indeed, the scaling relation (5.20), reformulated in terms of the free energy, can be written in the standard RG form

$$f_s \approx L^{-d} \mathcal{F} \left[M_0(T) h L^d, \frac{(n-1)k_B T}{\Upsilon(T)} L^{2-d}; r_{ij} \right], \quad (5.40)$$

where r_{ij} denote collectively various shape ratios. In this subsection we only specify L_{\parallel}/L explicitly. Recall, however, that even in the long cylinder geometry, there may also be some dependence on the *shape* of the cross-section, not only its area $A \equiv L^{d-1}$. Furthermore, \mathcal{F} is also n -dependent, beyond the factor $n-1$ shown explicitly.

Note that $M_0(T)$ and $\Upsilon^{-1}(T)$ play here the role of the “nonuniversal metric factors” discussed extensively in connection with the critical-point finite-size scaling. As in the Ising case, here also the irrelevant variable is dangerous. Due to a more conventional way of emergence of the RG scaling for $n > 1$ (*i.e.*, no L -dependence in the irrelevant scaling field), procedures of renormalizing down to a $1d$ chain of “giant” spins [112] do not have the ambiguities noted for the Ising ($n = 1$) case (Sect. 5.4.4).

5.5.2. Spin-Waves in Cubic Geometries

Scaling forms considered until now for n -vector models with $n = 1, 2, 3, \dots$ describe finite size rounding of the $\pm M_0$ jump in the (longitudinal) magnetization. For cubes, the jump is rounded on the H -scale $H_V \sim V^{-1}$, given by (5.4), while for long cylinders the rounding occurs on the scale $k_B T / M_0 A \xi_{\parallel} \sim A^{-2}$. However, additional finite-size effects will be present in both geometries on much larger H -scales, of order $\sim L^{-2}$. Indeed, for *bulk* vector-spin models below T_c , there is a divergent contribution, due to spin-waves, to the susceptibility in the $H \rightarrow 0^{\pm}$ limit, see, *e.g.*, [122]. The hydrodynamic (Gaussian) theory of spin wave fluctuations which, loosely, represent local rotations of the order parameter, has been reviewed in [107]. We only quote some results. The bulk correlation length behaves for small H according to

$$\xi^{(b)} \approx \sqrt{\Upsilon / M_0 |H|} \quad , \quad (5.41)$$

while the susceptibility has a singularity of the form

$$\chi_s^{(b)} \approx \text{const}(n - 1)k_B T(M_0/\Upsilon)^{d/2} |H|^{-(4-d)/2}, \quad (d > 2), \quad (5.42)$$

where const depends on d only, and an extra factor of $\ln |H|$ must be added in (5.42) for $d = 4, 6, 8, \dots$. This divergence (for $2 < d \leq 4$) results in the infinite slope of the magnetization as $H \rightarrow 0^\pm$.

Descriptions of the combined finite-size rounded first-order transition discontinuity and spin-wave singularities turn out to be rather complicated and have been considered in some detail only for (periodic) hypercubic or near hypercubic-shaped samples [107].

It was argued in [107] that the RG scaling expression (5.40) should apply in all regimes, with a more complicated dependence on the shape ratios r_{ij} and irrelevant-field argument $\sim TL^{2-d}$, see (5.40), than the form required to describe the leading-order (“jump”) rounding for cubes and cylinders. For “cubic” samples, three regimes can be identified.

a. Néel’s regime

As long as $|H| \leq O(H_V)$, so that the relevant scaling combination in (5.40) is not too large (it can be zero or up to $O(1)$ in magnitude), the dominant fluctuations are the “giant-spin” rotations. This can be viewed as the $\vec{k} = 0$ spin-wave mode (with no spatial orientation gradients) which is highly anharmonic for small hM_0V . In this regime the scaling functions for the magnetization, susceptibility, *etc.*, can be expanded in the irrelevant variable to yield Néel’s leading order results, *with spin-wave corrections* of relative magnitude L^{2-d} , with coefficients proportional to $(n - 1)k_B T/\Upsilon$. For the

susceptibility, this correction at $H = 0$ has been considered in some detail [107]. Thus, (5.11) is replaced (for $n > 1$) by

$$\chi(H = 0) = \frac{M_0^2}{n} V + \frac{(n-1)M_0^2 k_B T}{(n+2)\Upsilon} \text{const} L^2 + \dots, \quad (5.43)$$

where the (positive) const is geometry and possibly also n -dependent. (This and related results were established within a self-consistent scheme which becomes exact for $n = \infty$ [107].)

b. Spin-Wave Regime

For positive $hM_0V \gg 1$, the leading order expression (5.8) gives $M_s \approx M_0$. Expansion in the irrelevant variable acquires, however, a “dangerous” character. It turns out that to the first order in TL^{2-d} , one can write generally [107]

$$M_s \approx M_0 \left[m(hM_0V) + \frac{(n-1)k_B T L^{2-d}}{\Upsilon} m_1 \left(\frac{(n-1)HM_0L^2}{\Upsilon}; r_{ij} \right) \right]. \quad (5.44)$$

Thus, the function m_1 depends on the *product* ($\sim L^2$) of two scaling combinations and cannot be further expanded in the irrelevant combination $\sim TL^{2-d}$ in the regime where the relevant combination $\sim hL^d$ is large.

By (5.41), the new “product” scaling combination is proportional to $[L/\xi^{(b)}]^2$. Thus, for $hM_0V \gg 1$, when the first term in (5.44) becomes M_0 (*i.e.*, $m(+\infty) = 1$), the second term will vary for fields of order $\sim L^{-2}$, and it represents the rounding of the bulk

spin-wave singularities. This effect was observed in a MC study [123]. In this regime the $\vec{k} = 0$ spin-wave mode (“giant spin”) is frozen along the applied field. Fluctuations of the $\vec{k} \neq 0$ modes can be regarded harmonic and treated within a finite-size Gaussian model. Explicit results for the scaling functions like m_1 in (5.44) can then be obtained [107]. They are strongly geometry-dependent.

c. Intermediate Regime

When $|H| \ll O(L^{-2})$, and $|H|$ approaches values of order L^{-d} , the $\vec{k} = 0$ spin-wave mode is no longer frozen, and it interacts anharmonically with the $\vec{k} \neq 0$ modes. The resulting many-body problem cannot be analyzed except in the large- n limit. It has been conjectured [107] that (5.44) applies generally in the first order in TL^{2-d} , and a form of m_1 was proposed, valid to this order in all regimes.

Note that the rounded spin-wave susceptibility peak, of width $\sim L^{-2}$, reaches values of order $\sim L^{4-d}$ in this regime (see [107] for more detailed expressions), and smoothly crosses over to the “central” peak of width $\sim L^{-d}$ and maximal value given by (5.43).

5.5.3. Spherical Model Results

Spherical model calculations serve to test the general n -vector model predictions [107] outlined above (with properly rescaled factors of n), in the limit $n \rightarrow \infty$. Results have been obtained [113] for general cubic-like and cylindrical geometries in $d > 2$, as well as for long-range interactions decaying $\sim 1/R^{d+\sigma}$, with $0 < \sigma < 2$, for general $d > \sigma$. Note that $\sigma = 2$ corresponds to the short-range

case, and that for $\sigma < 2$, spin-wave concepts have not been formulated (for $n \leq \infty$) so that the scaling expressions are less physically transparent (see [113] for details).

Another extension achieved to date only for spherical models [124], are finite-size results for geometries other than cubic and cylindrical. General-geometry results obey the RG scaling, *e.g.*, (5.40); consult [124] for details.

5.4.4. Quantum Models

Several authors studied finite-size effects on first-order transitions in models where the order parameter is a quantum-mechanical vector operator. This recent development will not be reviewed here; see, *e.g.*, [125].

5.6. Nonsymmetric $n = 1$ Transitions

5.6.1. General Formulation

If \bar{k} distinct phases coexist, their (bulk) free energies are equal at the transition. Let us denote these free energies by $f_j^{(b)}(K_i)$, where $j = 1, 2, \dots, \bar{k}$, while K_i represent various thermodynamic fields (such as H, T) taking values $K_i^{(0)}$ at the transition. The mimic partition function for periodic cubes (we consider only this geometry here) is simply

$$\sum_{j=1}^{\bar{k}} e^{-V f_j^{(b)}(K_i)} . \quad (5.45)$$

While this result is easy to state, it is not that easily substantiated. There are actually two separate issues: (1) the meaning of $f_j^{(b)}(K_i \simeq K_i^{(0)})$ outside the part of the phase diagram where j is the stable phase (*i.e.*, where $f_j^{(b)}$ is minimal among the set $f_i^{(b)}$, at least, within mean-field theory); (2) the exponentials in (5.45) are added up with no coefficients. In order to avoid introduction of excessive notation, we will explore the above issues in the case $\bar{k} = 2$.

5.6.2. Two-Phase Coexistence

We turn again to magnetic type notation. Thus, we assume that the transition occurs when a certain “field” h equals zero. For *small* h , we assume that it couples to the order parameter Ψ , normalized in such a way that the Boltzmann factor due to this interaction (which is only a part of the total interaction energy density) is given by

$$\exp(h\Psi V). \quad (5.46)$$

At the phase transition the free energies of the coexisting phases can be expanded as

$$f_1^{(b)}(h) = f_0^{(b)} + M_1^{(b)}h + \frac{1}{2}\chi_1^{(b)}h^2 + \dots, \quad (5.47)$$

$$f_2^{(b)}(h) = f_0^{(b)} + M_2^{(b)}h + \frac{1}{2}\chi_2^{(b)}h^2 + \dots . \quad (5.48)$$

These series are asymptotic [126]. However, in finite-size analyses we usually need only a few terms and the resulting scaling expressions only involve the “spontaneous” values of $M_1^{(b)} > M_2^{(b)}$, etc. Thus, the issue of nonanalyticity of thermodynamic quantities as coexistence ($h = 0$) is approached, and their analytic continuation to the “metastable region”, are irrelevant.

When series (5.47)-(5.48) are substituted in (5.45), with $\bar{k} = 2$, the leading order finite-size scaling results can be easily calculated. For instance, for the magnetization we get

$$M_s \approx \frac{M_1^{(b)} + M_2^{(b)}}{2} + M_0 \tanh(hM_0V), \quad (\bar{k} = 2), \quad (5.49)$$

$$M_0 \equiv \left[M_1^{(b)} - M_2^{(b)} \right] / 2. \quad (5.50)$$

This simple result, reminiscent of the symmetric case, with no shift in the location of the transition, obviously relies strongly on the assumption (2) above, which was that the exponentials in (5.45) add up with no relative coefficients. Results (5.45) and (5.49)-(5.50) can be substantiated by exact and transfer matrix considerations which are briefly discussed in Sect. 5.6.4. A more detailed discussion will be based on the formalism of the probability density of the order parameter Ψ [108,127]. (We emphasize that the no-shift property is valid only for $\bar{k} = 2$.)

5.6.3. Probability Distribution of the Order Parameter

For convenience we assume the Ψ is a continuous scalar variable, taking values in $(-\infty, +\infty)$, which can be done without any loss of generality. The probability density distribution for Ψ , $P_L(\Psi) \equiv P_L(\Psi; T, h)$, is sharply peaked at the equilibrium “magnetization” M , and several studies [38,108] suggest that near M , it is Gaussian. The form usually assumed for $\Psi \simeq M$ is then

$$P_L(\Psi) \propto \exp \left[-\frac{(\Psi - M)^2}{2\chi} V \right], \quad (5.51)$$

where the width $\sim \sqrt{\chi/V}$ is a standard thermodynamic fluctuation result. Note that (5.51) is not normalized.

When $P_L(\Psi)$ is peaked at *two values*, $M_{1,2} = M_{1,2}^{(b)} + \chi_{1,2}^{(b)} h + \dots$, as happens at $h \simeq 0$, it is important to decide how to add up the peaks at M_1 and M_2 . The argument of [108] was essentially that one should add up *normalized* peaks so that away from phase coexistence, the dominant peak will yield normalized $P_L(\Psi)$. This line of argument leads to results equivalent to (5.45).

Another argument [127] is that $P_L(\Psi)$ must follow from the constrained fixed- Ψ zero-field free energy $p(\Psi; L)$, as

$$P_L(\Psi) = \frac{e^{-V[p(\Psi; L) - h\Psi]}}{\int_{-\infty}^{\infty} e^{-V[p(\psi; L) - h\psi]} d\psi} . \quad (5.52)$$

It is usually assumed that (5.51) follows from a minimum of $[p(\Psi; L) - h\Psi]$ at $\Psi = M$,

$$p - h\Psi \approx \frac{1}{2\chi}(\Psi - M)^2. \quad (5.53)$$

If there are two such minima in $p(\Psi; L)$ at $M_{1,2}^{(b)}$, it suggests that the correct approximation is to add up the exponentials *before* normalizing [127], which leads to results somewhat different from, *e.g.*, (5.49). However, note that this is a typical mean-field consideration. Usually, $p(\Psi; L)$ for $M_2^{(b)} < \Psi < M_1^{(b)}$ is corrected for multiphase effects [38] which are beyond mean-field theory. However, the normalization problem can be resolved if we also allow for rather mild finite-size modifications of $p(\Psi; L)$ beyond the strict mean-field type form. We can put, *e.g.*,

$$p - h\Psi \approx \frac{1}{2\chi}(\Psi - M)^2 - \frac{1}{2V} \ln \frac{V}{2\pi\chi}, \quad \text{for } \Psi \simeq M, \quad (5.54)$$

to get a normalized peak near $\Psi = M$ in the numerator of (5.52). Corrections of orders L^{-d} and $L^{-d} \ln L$ are not unusual for free energy quantities, although here they are not clearly associated with geometrical features. Thus, we can “normalize” the peaks at $M \simeq M_{1,2}^{(b)}$ by making the minima of p slightly unequal,

$$|\Delta p_{\min}| = \left| \frac{1}{2V} \ln \left(\chi_2^{(b)} / \chi_1^{(b)} \right) \right|, \quad (5.55)$$

resolving all the discrepancies.

5.6.4. Exact and Transfer Matrix Results

Recently, the general relation (5.45) has been established *rigorously* [128] within the Pirogov-Sinai theory of phase coexistence, which applies to a wide class of models at sufficiently low temperatures, see a review [129]. The $\bar{k} = 2$ result (5.49)-(5.50) has been also confirmed by transfer matrix considerations [130]. In fact, the original transfer matrix formulation [4] used the $H \leftrightarrow -H$ Ising symmetry only in relations like (5.47)-(5.48). Extension of the transfer matrix analysis to $\bar{k} > 2$ should also be possible.

5.7. Miscellaneous Topics

5.7.1. Matching of Scaling Forms

Several authors [4,34,51,107,131] considered a crossover from the critical-point scaling near T_c to the first-order transition scaling which sets up for $t < 0$ and $L \gg \xi^{(b)}$, *i.e.*, when $tL^{1/\nu}$ is large and negative. Thus, one can derive the asymptotic form of the critical-point scaling function $Y(\tau, \omega)$ for $\tau \rightarrow -\infty$, whenever explicit “first-order” scaling results are available (*e.g.*, [4,51]). We will not elaborate on specific results one of which [51] is relation (3.20). Instead, we comment of some points of general interest.

First, we note [4] that “first-order” scaling combinations depend on d . Thus, they can be put in the standard hyperuniversal scaling form only for $d < 4$. Specifically,

$$hM_0L^d \approx \frac{H}{k_B T_c} B_- |t|^\beta L^d \propto \left(H L^{\Delta/\nu} \right) |t L^{1/\nu}|^\beta L^{(d\nu-2+\alpha)/\nu}, \quad (5.56)$$

$$\sigma L^{d-1} \sim |t|^\mu L^{d-1} = |t L^{1/\nu}|^\mu L^{[(d-1)\nu-\mu]/\nu}, \quad (5.57)$$

$$(k_B T)^{-1} \Upsilon L^{d-2} \sim |t|^\nu L^{d-2} = |t L^{1/\nu}|^\nu L^{[(d-2)\nu-\nu]/\nu}, \quad (5.58)$$

where we introduced the helicity modulus exponent v , and used *scaling* relations $\Delta = \beta + \gamma$ and $\alpha + 2\beta + \gamma = 2$. Thus, (5.56)-(5.58) reduce to critical-point scaling combinations only if the standard hyperscaling relations can be used, $2 - \alpha = d\nu$ for (5.56), $\mu = (d-1)\nu$ for (5.57), and $v = (d-2)\nu$ for (5.58). In fact, matching of scaling forms has led to understanding of some of the aspects of modified finite-size behavior for $d > 4$ [4,34], see Sect. 2.7.

Another interesting property was found for spherical models [131] where it turns out that not only the scaling combinations near T_c and below T_c are compatible, but that a single *scaling function* can be used, see [131] for details. It has been speculated [131] that this property applies for all $n = 2, 3, \dots, \infty$. However, it is most likely restricted to models whose critical behavior is intrinsically Gaussian. These include the spherical model, but also in a certain sense the conformally invariant $2d$ models, where a similar effect (in the strip geometry) is the so-called Zamolodchikov's [132] c -theorem, see [133].

5.7.2. Extension to nonperiodic boundary conditions

Incorporation of surface effects in a systematic theory of finite-size rounded first-order transitions would be highly desirable, but no such development has been reported to date. Leading-order results (but not the form of the corrections) will remain unchanged for boundary conditions which (1) introduce no additional asymmetries, and (2) introduce no interfaces. For example, the Ising result (5.3) should apply also for free boundary conditions but not for, say, all + boundary conditions. In the latter case, a shift in h of order $1/L$ towards negative values will be needed. More qualitative changes should be expected for boundary conditions which induce interfaces [134].

5.7.3. Loci of Partition Function Zeros

In the complex- T or H planes, partition function zeros typically fall on line loci (with nonzero density). It has been pointed out [26,135] that these lines are reminiscent of first-order transitions in that in the bulk, the imaginary part of the free energy corresponds to discontinuous “order parameter” [135]. Furthermore, one can use relations of the type (5.45) to study the distribution of zeros in finite-size systems [26].

6. CONCLUSION

Overall, the theory of finite-size effects has been well developed. However, many topics still require theoretical work and numerical tests, notably surface and interfacial effects, applications to quantum systems, dynamics, and nonequilibrium phase transitions. The author hopes that this review has provided both an introduction and a survey of available results. However, he wishes to point out that many topics and results were left out or mentioned only in outline.

Acknowledgements

The author thanks his colleagues and collaborators, D.B. Abraham, M.C. Bartelt, K. Binder, J.L. Cardy, C.R. Doering, M.E. Fisher, G. Forgacs, G. Gaspari, M.L. Glasser, M. Nauenberg, M.P. Nightingale, R.K. Pathria, S. Redner, J. Rudnick, L.S. Schulman, N.M. Švrakić, A.M. Szpilka and A.P. Young for rewarding interactions. He also acknowledges support of his work by the United States National Science Foundation, and by the Donors of the Petroleum Research Fund, as well as a Graham research award.

REFERENCES

1. M.E. Fisher, in: *Critical Phenomena, Proc. 1970 E. Fermi Int. School of Physics*, M.S. Green ed. (Academic, NY, 1971), Vol. 51, p. 1.
2. M.N. Barber, in: *Phase Transitions and Critical Phenomena*,

- C. Domb and J.L. Lebowitz *eds.* (Academic, NY, 1983), Vol. **8**, p. 145.
3. M.P. Nightingale, *J. Appl. Phys.* **53**, 7927 (1982).
 4. V. Privman and M.E. Fisher, *J. Stat. Phys.* **33**, 385 (1983).
 5. E. Brézin and J. Zinn-Justin, *Nucl. Phys.* **B257[FS14]**, 867 (1985).
 6. K. Binder, *Ferroelectrics* **73**, 43 (1987) and *J. Comput. Phys.* **59**, 1 (1985).
 7. J.L. Cardy, in: *Phase Transitions and Critical Phenomena*, C. Domb and J.L. Lebowitz *eds.* (Academic, NY, 1987), Vol. **11**, p. 55.
 8. Reprint volume: *Finite-Size Scaling*, J.L. Cardy *ed.* (North-Holland, Amsterdam, 1988).
 9. V. Privman and M.E. Fisher, *Phys. Rev.* **B30**, 322 (1984).
 10. V. Privman, P.C. Hohenberg and A. Aharony, in: *Phase Transitions and Critical Phenomena*, C. Domb and J.L. Lebowitz *eds.* (Academic, NY, *in print*), see Ch. 10 there.
 11. M.E. Fisher, *Rev. Mod. Phys.* **46**, 597 (1974).
 12. M.E. Fisher and M.N. Barber, *Phys. Rev. Lett.* **28**, 1516 (1972).
 13. See also M.E. Fisher and A.E. Ferdinand, *Phys. Rev. Lett.* **19**, 169 (1967).
 14. E. Brézin, *J. Physique* **43**, 15 (1982).
 15. M.P. Nightingale and H.W.J. Blöte, *J. Phys. A* **16**, L657 (1983).
 16. J. Rudnick, H. Guo and D. Jasnow, *J. Stat. Phys.* **41**, 353

- (1985).
17. A.M. Nemirovsky and K.F. Freed, J. Phys. A**18**, L319 (1985) and A**19**, 591 (1986).
 18. H. Guo and D. Jasnow, Phys. Rev. B**35**, 1846 (1987), see also Jasnow's article in this volume.
 19. B. Widom, J. Chem. Phys. **43**, 3898 (1965).
 20. D. Stauffer, M. Ferer and M. Wortis, Phys. Rev. Lett. **29**, 345 (1972).
 21. F. Wegner, Phys. Rev. B**5**, 4529 (1972).
 22. V. Privman and M.E. Fisher, J. Phys. A**16**, L295 (1983); V. Privman, Physica **123A**, 428 (1984); H.J. Hermann and D. Stauffer, Phys. Lett. **100A**, 366 (1984); B. Derrida and D. Stauffer, J. Physique **46**, 1623 (1985).
 23. A. Aharony and M.E. Fisher, Phys. Rev. B**27**, 4394 (1983).
 24. S.I. Chase and M. Kaufman, Phys. Rev. B**33**, 239 (1986).
 25. V. Privman and J. Rudnick, J. Phys. A**19**, L1215 (1986).
 26. M.L. Glasser, V. Privman and L.S. Schulman, Phys. Rev. B**35**, 1841 (1987).
 27. V. Privman, Phys. Rev. B**38**, 9261 (1988).
 28. J.L. Cardy and I. Peschel, Nucl. Phys. B**300** [FS**22**], 377 (1988).
 29. P.-Y. Lai and K.K. Mon, Phys. Rev. B, *in print*.
 30. K. Symanzik, Nucl. Phys. B**190**[FS**3**], 1 (1981).
 31. E. Eisenriegler, Z. Physik B**61**, 299 (1985).
 32. V. Dohm, Z. Physik B**75**, 109 (1989).

33. K.K. Mon and M.P. Nightingale, Phys. Rev. **B31**, 6137 (1985), and references therein. See also Mon's article in this volume.
34. K. Binder, M. Nauenberg, V. Privman and A.P. Young, Phys. Rev. **B31**, 1498 (1985).
35. M.E. Fisher, In: *Renormalization Group in Critical Phenomena and Quantum Field Theory*, J.D. Gunton and M.S. Green eds. (Temple University, Philadelphia), p. 65.
36. J. Rudnick, G. Gaspari and V. Privman, Phys. Rev. **B32**, 7594 (1985).
37. R.C. Desai, D.W. Heermann and K. Binder, J. Stat. Phys. **53**, 795 (1988).
38. K. Binder, Z. Physik **B43**, 119 (1981) and Phys. Rev. Lett. **47**, 693 (1981).
39. E. Eisenriegler and R. Tomaschitz, Phys. Rev. **B35**, 4876 (1987).
40. K. Binder and J.-S. Wang, J. Stat. Phys., *in print*, see also Binder's article in this volume.
41. V. Privman and N.M. Švrakić, *Directed Models of Polymers, Interfaces, and Clusters: Scaling and Finite-Size Properties*, Lecture Notes in Physics **338** (Springer-Verlag, Berlin, 1989).
42. Y.Y. Goldschmidt, Nucl. Phys. **B280[FS18]**, 340 (1987) and **B285[FS19]**, 519 (1987); H.W. Diehl, Z. Physik **B66**, 211 (1987); C.R. Doering and M.A. Burschka, *preprint*.
43. W. Vogelsberger, J. Colloid Interface Sci. **103**, 448 (1985); K.K. Mon and D. Jasnow, Phys. Rev. Lett. **59**, 2983 (1987); J. Viñals and D. Jasnow, Phys. Rev. **B37**, 9582 (1987).

44. A.D. Bruce, J. Phys. **A18**, L873 (1985).
45. K. Kaski, K. Binder and J.D. Gunton, Phys. Rev. **B29**, 3996 (1984).
46. M.N. Barber, R.B. Pearson, D. Toussaint and J.L. Richardson, Phys. Rev. **B32**, 1720 (1985).
47. A. Sariban and K. Binder, J. Chem. Phys. **86**, 5859 (1987).
48. T.W. Burkhardt and B. Derrida, Phys. Rev. **B32**, 7273 (1985).
49. K.G. Wilson, Phys. Rev. B4, 3174 and 3184 (1971).
50. A.D. Bruce, J. Phys. **C14**, 3667 (1981).
51. V. Privman, Physica **129A**, 220 (1984).
52. H. Saleur and B. Derrida, J. Physique **46**, 1043 (1985).
53. J.L. Cardy, J. Phys. **A17**, L385 (1984).
54. J.L. Cardy, Nucl. Phys. **B240[FS12]**, 514 (1984).
55. B. Derrida, B.W. Southern and D. Stauffer, J. Physique **48**, 335.
56. A.B. Harris, J. Phys. **C7**, 1671 (1974).
57. V. Privman and L.S. Schulman, J. Stat. Phys. **29**, 205 (1982) and J. Phys. **A15**, L231 (1982).
58. S. Singh and R.K. Pathria, Phys. Rev. **B31**, 4483 (1985). See also J. Shapiro and J. Rudnick, J. Stat. Phys. **43**, 51 (1986). For earlier finite-size studies of the spherical models, see M.N. Barber and M.E. Fisher, Ann. Phys. (NY) **77**, 1 (1973).
59. S. Singh and R.K. Pathria, Phys. Rev. **B32**, 4618 (1985).
60. S. Singh and R.K. Pathria, Phys. Rev. **B31**, 1816 (1985) and **B35**, 4814 (1987).

61. S. Singh and R.K. Pathria, Phys. Rev. **B38**, 2740 (1988), and references therein.
62. H.E. Stanley, Phys. Rev. **176**, 718 (1968).
63. J.M. Luck, Phys. Rev. **B31**, 3069 (1985).
64. M. Henkel, J. Phys. **A21**, L227 (1988).
65. K.K. Mon, Phys. Rev. Lett. **54**, 2672 (1985).
66. M. Henkel, J. Phys. **A19**, L247 (1986).
67. M. Henkel, J. Phys. **A20**, L769 (1987).
68. M. Henkel, J. Phys. **A20**, 3669 (1987).
69. M. Henkel, J. Phys. **A20**, 995 (1987).
70. J.O. Indekeu, M.P. Nightingale and W.V. Wang, Phys. Rev. **B34**, 330 (1986).
71. J.O. Indekeu, J. Chem. Soc. *Faraday Trans. II*, **82**, 1835 (1986); K.K. Mon and M.P. Nightingale, Phys. Rev. **B35**, 3560 (1987).
72. Reprint volume: *Conformal Invariance and Applications to Statistical Mechanics*, C. Itzykson, H. Saleur and J.-B. Zuber eds. (World Scientific, Singapore, 1988).
73. J.L. Cardy, Nucl. Phys. **B275[FS17]**, 200 (1986).
74. T.W. Burkhardt and I. Guim, Phys. Rev. **B35**, 1799 (1987).
75. J.-M. Debierre and L. Turban, J. Phys. **A20**, 1819 (1987), and references therein.
76. V. Privman and S. Redner, J. Phys. **A18**, L781 (1985).
77. H.W.J. Blöte, J.L. Cardy and M.P. Nightingale, Phys. Rev. Lett. **56**, 742 (1986). See also I. Affleck, Phys. Rev. Lett. **56**,

- 746 (1986).
78. A.E. Ferdinand and M.E. Fisher, Phys. Rev. **185**, 832 (1969).
 79. M.E. Fisher and H. Au-Yang, Physica **101A**, 255 (1980); H. Au-Yang and M.E. Fisher, Phys. Rev. B**11**, 3469 (1975) and B**21**, 3956 (1980).
 80. H. Park and M. den Nijs, Phys. Rev. B**38**, 565 (1988).
 81. K.K. Mon and D. Jasnow, Phys. Rev. A**30**, 670 (1985).
 82. D.B. Abraham and N.M. Švrakić, Phys. Rev. Lett. **56**, 1172 (1986).
 83. D. Jasnow, K.K. Mon and M. Ferer, Phys. Rev. B**33**, 3349 (1986).
 84. L. Onsager, Phys. Rev. **65**, 117 (1944).
 85. V. Privman, *preprint*.
 86. N.M. Švrakić, V. Privman and D.B. Abraham, J. Stat. Phys. **53**, 1041 (1988).
 87. D.B. Abraham, *preprint*.
 88. V. Privman, Phys. Rev. Lett. **61**, 183 (1988).
 89. M.P. Gelfand and M.E. Fisher, Int. J. Thermophysics **9**, 713 (1988).
 90. R. Lipowsky and G. Gompper, Phys. Rev. B**29**, 5213 (1984).
For related results, see B. Legait and P.G. de Gennes,
J. Physique Lett. **45**, L-647 (1984); R. Evans and U.M.B. Marconi, J. Chem. Soc. *Faraday Trans. II*, **82**, 1763 (1986).
 91. M.P. Gefand and R. Lipowsky, Phys. Rev. B**36**, 8725 (1987);
J.O. Indekeu, P. Upton and J. Yeomans, Phys. Rev. Lett.

- 61, 2221 (1988) and Phys. Rev. B40, 666 (1989). For related results, see also R.J. Creswick, H.A. Farach and C.P. Poole, Jr., Phys. Rev. B35, 8467 (1987).
92. D.M. Kroll and G. Gompper, Phys. Rev. B39, 433 (1989).
 93. V. Privman and N.M. Švrakić, Phys. Rev. B37, 3713 (1988).
 94. G. Forgacs, N.M. Švrakić and V. Privman, Phys. Rev. B37, 3818 (1988) and B38, 8996 (1988).
 95. J. Stecki and J. Dudowicz, Proc. R. Soc. Lond. A400, 263 (1985).
 96. M.E. Fisher and D.S. Fisher, Phys. Rev. B25, 3192 (1982).
 97. V. Privman and N.M. Švrakić, J. Stat. Phys. 54, 735 (1989) and Phys. Rev. Lett. 62, 633 (1989).
 98. J. Bricmont, A. El Mellouki and J. Fröhlich, J. Stat. Phys. 42, 743 (1986).
 99. G.G. Cabrera and R. Jullien, Phys. Rev. Lett. 57, 393 and 3297 (1986), and Phys. Rev. B35, 7062 (1987); J. Zinn-Justin, Phys. Rev. Lett. 57, 3296 (1986); M.N. Barber and M.E. Cates, Phys. Rev. B36, 2024 (1987); D.B. Abraham, L.F. Ko and N.M. Švrakić, Phys. Rev. Lett. 61, 2393 (1988) and J. Stat. Phys. *in print*.
 100. M.E. Fisher, J. Phys. Soc. Japan Suppl. 26, 87 (1969).
 101. G. Münster, *preprint* (DESY-89-011).
 102. K.K. Mon, S. Wansleben, D.P. Landau and K. Binder, Phys. Rev. Lett. 60, 708 (1988) and Phys. Rev. B39, 7089 (1989).
 103. G.A. Williams, Japan. J. Appl. Phys. 26, Suppl. 26-3, 305

- (1987); K.Y. Szeto and G. Dresselhaus, Phys. Rev. B**32**, 3142 (1985).
104. B. Nienhuis and M. Nauenberg, Phys. Rev. Lett. **35**, 477 (1975); M.E. Fisher and A.N. Berker, Phys. Rev. B**26**, 2507 (1982).
105. K. Binder, Rep. Prog. Phys. **50**, 783 (1987); see also Bhanot's and Landau's articles in this volume.
106. M.S.S. Challa, D.P. Landau and K. Binder, *preprint*.
107. M.E. Fisher and V. Privman, Phys. Rev. B**32**, 447 (1985).
108. K. Binder and D.P. Landau, Phys. Rev. B**30**, 1477 (1984).
109. C. Dasgupta and B.I. Halperin, Phys. Rev. Lett. **47**, 1556 (1981).
110. L. Néel, C. R. Acad. Sci. **228**, 664 (1949); Ann. Géophys. **5**, 99 (1949).
111. I.S. Jacobs and C.P. Bean, in *Magnetism*, G.T. Rado and H. Suhl *eds.* (Academic, NY, 1963), Vol. III, p. 271.
112. J.L. Cardy and P. Nightingale, Phys. Rev. B**27**, 4256 (1983); H.W.J. Blöte and M.P. Nightingale, Physica **112A**, 405 (1982); see also Barber's review [2].
113. M.E. Fisher and V. Privman, Com. Math. Phys. **103**, 527 (1986).
114. This mechanism of absence of ordering in $1d$ systems is credited to L.D. Landau: see L.D. Landau and E.M. Lifshitz, *Statistical Physics*, Theoretical Physics, Vol. V (Science, Moscow, 1964, *in Russian*), Sect. 152.

115. C.J. Hamer and C.H.J. Johnson, J. Phys. A**19**, 423 (1986).
116. V. Privman and M.E. Fisher, J. Appl. Phys. **57**, 3327 (1985).
117. D.B. Abraham, Stud. Appl. Math. **50**, 71 (1971).
118. Numerical results in $4d$, were reported by K. Jansen, J. Jersák, I. Montvay, G. Münster, T. Trappenberg and U. Wolff, Phys. Lett. **213B**, 203 (1988); K. Jansen, I. Montvay, G. Münster, T. Trappenberg and U. Wolff, *preprint* (DESY-88-169).
119. G.G. Cabrera, R. Jullien, E. Brézin and J. Zinn-Justin, J. Physique **47**, 1305 (1986).
120. V. Privman and M.E. Fisher, J. Magn. Magnet. Mater. **54-57**, 663 (1986).
121. M.E. Fisher, *unpublished* (1973).
122. M.E. Fisher, M.N. Barber and D. Jasnow, Phys. Rev. A**8**, 1111 (1973); A.L. Patashinskii and V.L. Pokrovskii, Zh. Eksp. Teor. Fiz. **64**, 1445 (1973) [Sov. Phys. JETP **37**, 733 (1974)].
123. H. Müller-Krumbhaar, Z. Physik **267**, 261 (1974), studied $3d$ Heisenberg ($n = 3$) systems of up to 16^3 spins.
124. S. Singh and R.K. Pathria, Phys. Rev. B**37**, 7806 (1988).
125. H. Neuberger and T. Ziman, Phys. Rev. B**39**, 2608 (1989); D.S. Fisher, Phys. Rev. B**39**, 11783 (1989).
126. S.N. Isakov, Com. Math. Phys. **95**, 427 (1984). For additional literature, see [57].
127. M.S.S. Challa, D.P. Landau and K. Binder, Phys. Rev. B**34**, 1841 (1986).
128. C. Borgs and R. Kotecký, *work in progress*.

129. C. Borgs and J. Imbrie, Com. Math. Phys. **123**, 305 (1989).
130. M.E. Fisher, *unpublished notes*.
131. S. Singh and R.K. Pathria, Phys. Rev. **B34**, 2045 (1986), see also [124].
132. A.B. Zamolodchikov, Pisma Zh. Eksp. Teor. Fiz. **43**, 565 (1986) [JETP Lett. **43**, 730 (1986)].
133. D. Boyanovsky and C.M. Naon, *preprint*.
134. J.H. Mayer and W.W. Wood, J. Chem. Phys. **42**, 4268 (1965); M.C. Bartelt and V. Privman, *work in progress*.
135. C. Itzykson, R.B. Pearson and J.-B. Zuber, Nucl. Phys. **B220**, 415 (1983).